We acknowledge Dr. J. D. Garrett for his assistance with the gas target and Dr. R. Middleton for several interesting discussions. We also acknowledge Mrs. Joann Hoffman for her careful scanning of the nuclear emulsion plates. One of us (H.T.F.) acknowledges several interesting discussions with Dr. R. D. Lawson, who in fact suggested using the ^{40}Ar(^{6}Li, d) reaction to investigate the 6p-2h nature of states in ^{44}Ca.

---

*Work supported by the National Science Foundation.

[1]P. Federman and S. Pittel, Nucl. Phys. A155, 161 (1970).

[2]J. B. McGrory, B. H. Wildenthal, and E. C. Halbert, Phys. Rev. C 2, 186 (1970).

[3]R. D. Lawson, private communication.

[4]See, for example, K. Meier-Ewert, K. Bethge, and K.-O. Pfeiffer, Nucl. Phys. A110, 142 (1968). See also G. Brommundt, H. G. Ritter, R. Bock, and F. Puhlhofer, in *Proceedings of the International Conference on Nuclear Reactions Induced by Heavy Ions, Heidelberg, Germany, 15–18 July 1969,* edited by R. Bock and W. R. Hering (North-Holland Publishing Company, Amsterdam, The Netherlands, 1970), p. 293.

[5]R. Middleton, in *Proceedings of the International Conference on Nuclear Reactions Induced by Heavy Ions, Heidelberg, Germany, 15–18 July 1969,* edited by R. Bock and W. R. Hering (North-Holland Publishing Company, Amsterdam, The Netherlands, 1970), p. 263.

[6]K. Bethge, C. M. Fou, and R. W. Zurmuhle, Nucl. Phys. A123, 521 (1969).

[7]H. T. Fortune, N. G. Puttaswamy, and J. L. Yntema, Phys. Rev. 185, 1546 (1969).

[8]J. H. Bjerregaard and O. Hansen, Phys. Rev. 155, 1229 (1967).

PHYSICAL REVIEW C VOLUME 4, NUMBER 3 SEPTEMBER 1971

Distorted-Wave Born-Approximation Analysis of the ^{90}Zr(d, α)^{88}Y and ^{89}Y(^{3}He, α)^{88}Y Reactions

Yong Sook Park, H. D. Jones, and D. E. Bainum
U. S. Army Ballistic Research Laboratories, Aberdeen Proving Ground, Maryland 21005

(Received 10 February 1971)

The levels of ^{88}Y have been studied with the ^{90}Zr(d, α) and ^{89}Y(^{3}He, α) reactions with 30- to 40-keV resolution at 15-MeV incident energy. The (d, α) angular distributions for transitions to eight prominent levels below 2.2 MeV have been measured over $15° \leq \theta \leq 150°$. The reliability of parameters entering distorted-wave Born-approximation calculations was checked in detail. The (d, α) calculations include the finite-range correction of Chant and Mangelson. The two-nucleon form factors (f.f.) were generated by the oscillator-expansion technique of Drisko and Rybicki, and the effect of residual interaction on the f.f. and angular distributions was studied. An attempt has been made to determine the (d, α) absolute normalization constant based on local zero-range calculations, and limits of $20 \leq D_0^2 \leq 30$ have been set. Two-nucleon f.f. generated by the Bayman-Kallio method were compared with the Drisko-Rybicki f.f. The (^{3}He, α) angular distributions for eight strongly populated levels below 1.7 MeV were measured over $20° \leq \theta \leq 125°$. Spectroscopic factors and l_n transfers have been extracted with both local zero-range and nonlocal finite-range calculations. The (^{3}He, α) results were compared with (d, α) results to determine unique parities and narrow J^π limits for the levels studied. ^{3}He and α elastic scattering on ^{89}Y have also been measured and optical-model potentials have been determined. Good agreement between this work and the recently reported ^{85}Rb($\alpha, n\gamma$)^{88}Y results is seen for the level energy and J^π assignments made.

I. INTRODUCTION

Direct (d, α) reactions on 0^+ targets have proved to be powerful tools with which to investigate the spectroscopy of odd-odd nuclei when the reactions are compared with single-particle-transfer reactions feeding the same final nucleus.[1] The reliability of spectroscopic information extracted from the measured (d, α) angular distributions depends largely on parameters entering in the current distorted-wave Born-approximation (DWBA) calculations of two-nucleon-transfer reactions.[2,3] The inclusion of the nonlocality and finite-range corrections into the conventional local zero-range DWBA calculations for (d, α) transitions has helped to bring the calculations into closer agree-

ment with the data.[1] The corrections normally employed are based on the local-energy approximation (LEA).[4] The justification for employing the LEA corrections in the two-nucleon-transfer case involves the assumption of a deuteron cluster for the transferred pair of nucleons; but we demonstrate in this work that the cluster formalism is not, in general, an accurate substitute for the microscopic formalism of two-nucleon form factors (f.f.).

The finite-range effect due to the nucleon-nucleon residual interaction has long been ignored in the DWBA treatment of two-nucleon-transfer reactions, and this effect is usually replaced by the zero-range approximation.[2,3] Recently, Chant and Mangelson[5] have formulated a method, in conjunction with the oscillator-expansion technique of Drisko and Rybicki,[6] by which the finite-range effects due to both the spatial separation of the transferred nucleons and the residual interaction can be properly treated. It has just been reported that the use of this finite-range correction in the DWBA calculations for the ^{52}Cr$(d, \alpha)^{50}$V reaction has enhanced the reproducibility of the data far more than does the use of the LEA cluster finite-range correction.[7] However, the above calculations ignored the effect of the residual interaction on the two-nucleon f.f. The zero-range f.f. are modified when this interaction is taken into account.[5] In this paper we test the validity of the method of Chant and Mangelson in detail in the DWBA analysis of the ^{90}Zr$(d, \alpha)^{88}$Y reaction by comparing calculations based on two-nucleon f.f. (with and without the inclusion of the residual interaction) with measured (d, α) angular distributions. The calculations based on the Chant-Mangelson finite-range correction are also compared with those based on the LEA correction.

It has been observed that the accuracy of DWBA results for direct (d, α) transitions is critically dependent upon the selection of the proper optical potentials for the α channel.[1] Since no such α-potential set pertinent to the present ^{90}Zr(d, α) study exists in the literature, it was necessary to measure the α elastic scattering. Three α-potential sets have been searched from this data. Standard procedures were used to derive a unique set to be used in the ^{90}Zr(d, α) analysis.[1]

The ^{89}Y$(^3$He, $\alpha)^{88}$Y reaction has previously been studied at 18 MeV by Fou and Zurmühle[8] as well as by Bassani and Picard.[9] Due to poor energy resolution (60–80 keV) obtained in both experiments, the levels beyond 1-MeV excitation of ^{88}Y remained unresolved, and the level energy assignments for them are uncertain. In addition, the reliability of the DWBA calculations employed in their work is somewhat uncertain because they were local zero-range calculations based on optical-potential parameters which were obtained for different energies and masses than those involved in their experiments. We have studied the ^{89}Y$(^3$He, $\alpha)$ reaction with improved resolution of 30 to 40 keV, and as a result more reliable assignments of level energies l_n and j_n values were possible. The ^{3}He optical-model potential relevant to the present reaction has been searched from the measured elastic scattering and utilized in the calculations. The sensitivity of DWBA calculations to parameter variations has been studied to ensure reliable extraction of spectroscopic information from our data.

The preliminary results on the spectroscopic study of the low-lying levels of ^{88}Y based solely on the analysis of the ^{90}Zr(d, α) reaction have already been reported by us.[10] A more comprehensive investigation of the level structure of ^{88}Y has been attempted here from the results of both the ^{90}Zr(d, α) and ^{89}Y$(^3$He, $\alpha)$ reactions and analysis based on more-refined DWBA calculations. The complete wave functions pertinent to the present (d, α) reaction are not available; hence the usefulness of a (d, α) reaction in checking the validity of the nuclear wave functions of the target, as well as the final states, has not been tested in this paper.

II. EXPERIMENTAL PROCEDURES AND RESULTS

A. ^{90}Zr$(d, \alpha)^{88}$Y and ^{89}Y$(^3$He, $\alpha)^{88}$Y Reactions

The (d, α) angular distributions were measured with 15-MeV incident deuterons from the Nuclear Effects Laboratory (NEL) tandem accelerator over the angular range of $15^\circ \leq \theta_L \leq 150^\circ$. A detailed description of the scattering facilities and the detection system used in this experiment is given in Ref. 11. α particles were detected with an array of four 300-μ-thick silicon surface-barrier detectors which were cooled to -30°C. Changes in target thickness, target angle, and beam-charge collection were monitored by detecting elastically scattered particles with a 2-mm-thick surface-barrier detector at a fixed angle of -80°. The target was 99% enriched ^{90}Zr isotope evaporated onto a 20-μg/cm^2-thick carbon backing, and its thickness was about 60 μg/cm^2.

An α-particle energy spectrum is shown in Fig. 1. The resolution obtained was about 30 keV for 20-MeV α particles. A comparison with a high-resolution spectrum taken with 15-keV resolution[12] reveals that some levels beyond 1-MeV excitation remain unresolved in this experiment. Angular distributions were thus obtained for only eight well-resolved prominent levels below 2.2-MeV excita-

tion in ^{88}Y. The levels are labeled with the excitation energies assigned in the present experiment. Accurate energy assignments for levels above 1 MeV had not been made prior to the initiation of this work. The level energies were determined from the known energies of ^{25}Mg and ^{26}Al levels populated in ^{27}Al(d, α) and ^{27}Al$(^3$He, $\alpha)$ reactions, respectively. Assigned values in Fig. 1 are weighted averages of values determined in both ^{90}Zr(d, α) and ^{89}Y$(^3$He, $\alpha)$ reactions. They are accurate to within ±5 keV except for those in parentheses, where ±10 keV is claimed. Arrows indicate the locations of levels below 1 MeV seen in other reactions, but not populated in the present (d, α) reaction, because they are inhibited by (d, α) selection rules.

The cross sections were obtained from the monitored deuteron elastic counts and the known deuteron elastic scattering cross section at the monitor angle and the incident energy.[13] The measured (d, α) angular distributions for transitions to the eight levels of ^{88}Y are labeled by the excitation energies and compared with the results of DWBA calculations as shown in Figs. 9 and 19. Angular distributions for the imperfectly resolved levels at 1.279 and 1.326 MeV were obtained with the aid of a computerized fitting program.[14]

Angular distributions for the $(^3$He, $\alpha)$ reaction were measured at 15 MeV over the angular range of $20° \leq \theta_L \leq 125°$. The experimental setup used was the same as that for the (d, α) experiment. The target was about 150 μg/cm^2 thick and was prepared by the evaporation of natural yttrium metal on a 30-μg/cm^2-thick carbon backing.[15] A typical ^{89}Y$(^3$He, $\alpha)$ energy spectrum is shown in Fig. 2. No prominent levels are seen beyond 2-MeV excitation. This does not appear to be a result of the relatively low incident energy employed in this experiment since the previous investigations of this reaction[8,9] conducted at 18 MeV also manifest this phenomenon. It is interesting to compare the $(^3$He, $\alpha)$ spectrum with that of the (d, α) reaction in Fig. 1, where levels of moderate strength are populated even to 3 MeV. The $(^3$He, $\alpha)$ reaction angular distributions were obtained for transitions to eight strongly populated levels up to 1.7 MeV. They are shown in Figs. 6 and 7, where they are compared with DWBA calculations to be described later. Angular distributions for the two imperfectly resolved levels at about 1.2-MeV excitation were again obtained with the aid of a fitting program.[14] A combined angular distribution was obtained for the unresolved doublet at 1.5 MeV. Both members are believed to be populated by $l_n = 1$ transfer.[8,9]

The dominant reaction mechanism for both the (d, α) and $(^3$He, $\alpha)$ reactions on targets in the mass-90 region at 15-MeV incident energy is expected to be a direct one-step process. This is strongly supported by the observation that the well-known 0^+ state at 0.77 MeV is strongly populated in the $(^3$He, $\alpha)$ and (p, d) neutron-pickup reactions,[8,9,16]

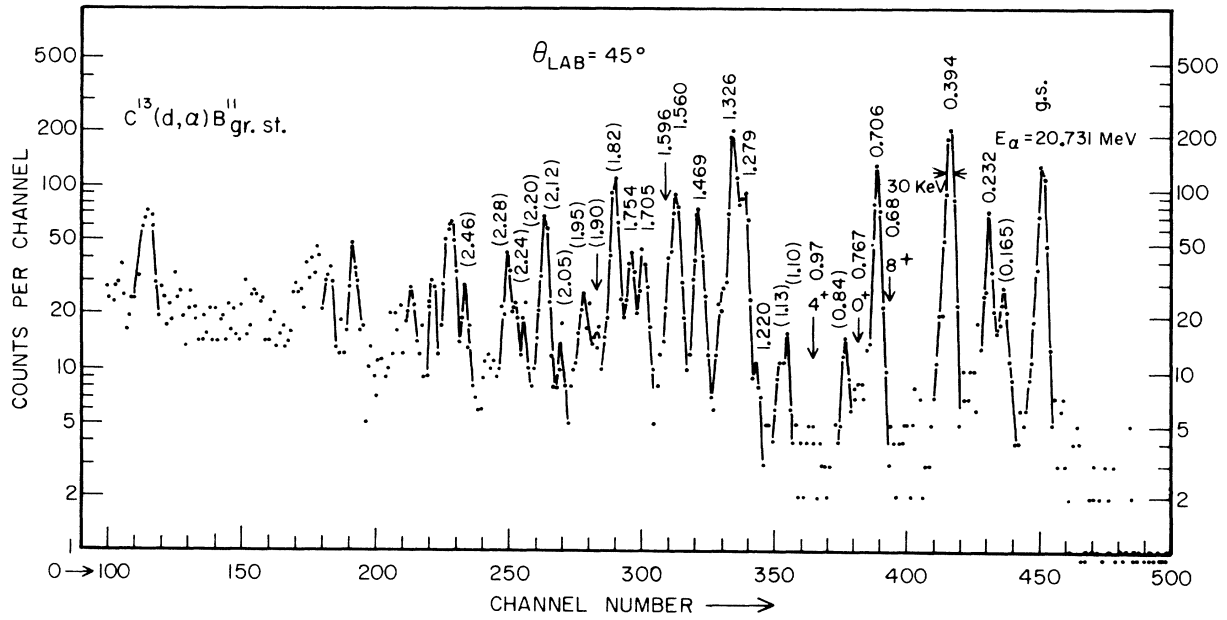

FIG. 1. α spectrum from the ^{90}Zr(d, α) reaction. Levels of ^{88}Y are identified by their measured excitation energies. The arrows below 1 MeV indicate the expected locations of levels reported in other reactions, but not seen in (d, α), because of its selective nature.

but is either not populated or very weakly populated in our (d, α) reaction (compare Figs. 1 and 2). Transitions from 0^+ to 0^+ states are prohibited in a direct one-step (d, α) reaction.

B. ^{89}Y(^{3}He, ^{3}He) and ^{89}Y(α, α) Experiments

The ^{89}Y(α, α) angular distribution was measured at 20 MeV from 15 to 130° in steps of 2.5°. Although the (^{3}He, α) angular distributions were measured at 15 MeV, it was deemed necessary to measure the ^{3}He elastic scattering at an energy sufficiently higher than the Coulomb-barrier potential in order to extract physically meaningful ^{3}He optical-model-potential sets for the DWBA analysis of the data. Hence the ^{3}He elastic scattering angular distributions were measured at 20 MeV as well as 15 MeV from 15 to 150°.

The experimental setup was basically identical to that for the (d, α) and (^{3}He, α) runs. The yttrium target exposed in the (^{3}He, α) run was used. The angular-distribution measurements were repeated twice to check the reproducibility of the data points, and the two sets of data agreed within 5%. Weighted averages of the two cross sections were adopted as the final values. Absolute cross-section scales were fixed by the best overall fit of the relative angular distributions, obtained on the basis of the monitored elastic counts, to the cross sections obtained on the basis of the beam charge times the target thickness. The target thickness (150 μg/cm^2) quoted earlier was determined from the measurement of the Coulomb scattering at forward angles. The measured α and ^{3}He angular distributions at 20 MeV are shown in Fig. 3, in which the ratios $d\sigma/d\sigma_{\text{Ruth}}$ are plotted. The curves represent the results of the optical-model parameter searches, for which the procedure will be described later.

C. Experimental Errors in Cross Sections

The true beam zero position was determined by measuring and comparing elastically scattered particles at small positive and negative forward angles. The deviation between the beam direction and the zero angle of the turntable was typically ±0.1°.

The random errors are represented by error bars on the individual data points on all measured angular distributions. They are primarily due to counting statistics, background subtractions, am-

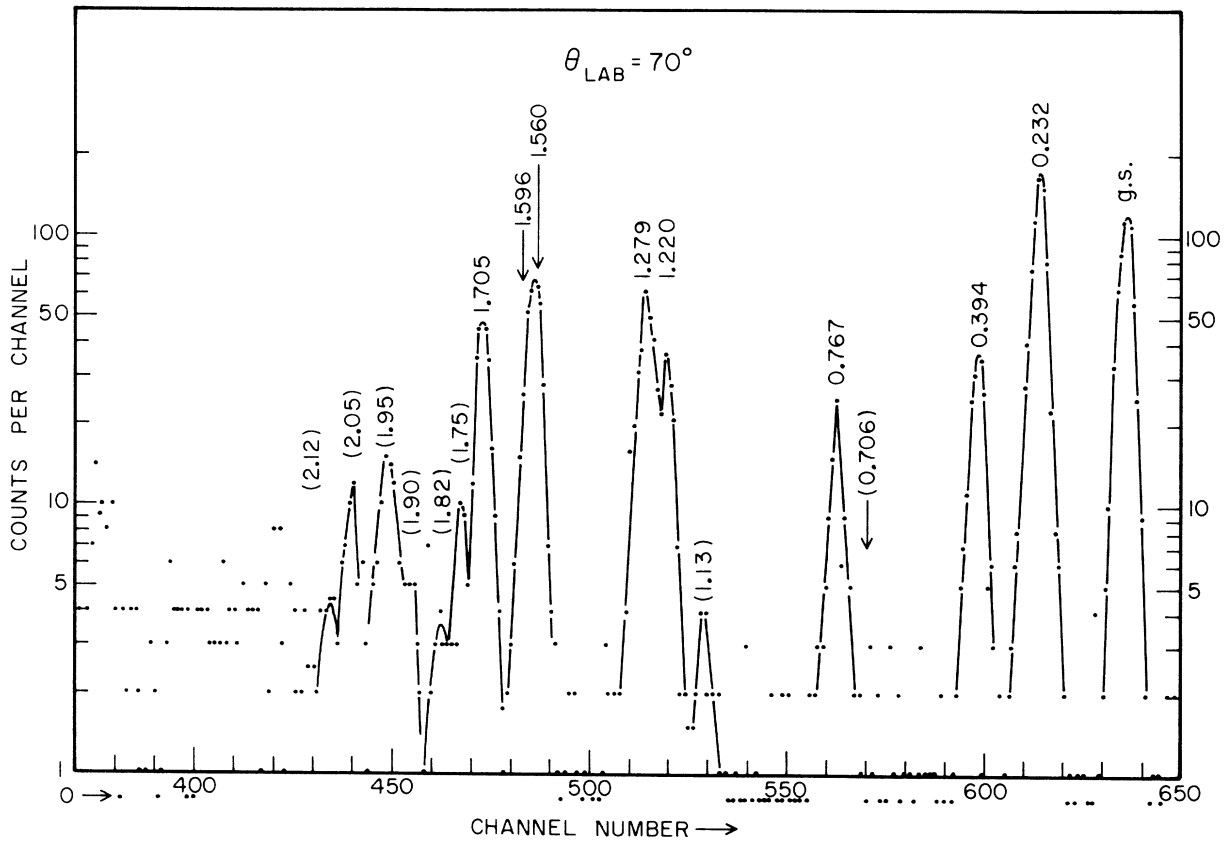

FIG. 2. α spectrum from the ^{89}Y(^{3}He, α) reaction.

biguities associated with the graphical analysis of imperfectly resolved adjacent peaks, and uncertainties in the relative solid angles of the four detectors used in measuring the relative angular distributions. Uncertainties of the latter type were estimated to be ±2%, a value determined from measuring the cross sections at the same angles by different detectors having different solid angles.

The dominant contributions to the absolute reaction cross-section errors came from uncertainties in the elastic scattering cross sections at the monitor angle. These uncertainties are in turn dependent on the target thickness. Significant contributions to the absolute reaction cross-section errors are listed as follows:
(i) error in the elastic scattering absolute cross sections: ±10%,
(ii) error in the monitor angle ($\Delta\theta \leq \pm 1^\circ$): ±5%,
(iii) error in the monitor-counter solid angle: ±5%.
The over-all cross-section errors are estimated to be ±13%.

III. THEORETICAL CONSIDERATIONS AND DWBA ANALYSIS

A. ^{3}He and α Optical-Model-Potential Parameter Search

It is known that considerable ambiguities exist in the parameter values for the optical-model-potential fits to the scattering of strongly absorbed particles such as α particles.[17] Two types of ambiguities may be distinguished. First, a small change in the value of one parameter may be compensated for by a small change in one or more other parameters. The second type of ambiguity results from the existence of a family of discrete parameter sets which give equally good scattering cross sections. Furthermore, it is known that the different sets belonging to the same family for the composite particles give rise to different results in the DWBA calculations[18] for reactions such as (d, α)[1] and (^{3}He, α).[19] It is then imperative that the proper potential set be used in the DWBA calculations before spectroscopic studies can be made with confidence. Since ^{3}He and α-potential sets relevant to the present reactions did not exist in the literature, they were searched from the elastic scattering angular distributions measured at this laboratory. Since the principal goal of this study is not the extraction of optical parameters, only a brief summary will be given of the search procedure. (A detailed account of the procedure will be given in Ref. 11.)

Parameters found in recent literature for nuclei and energies which are as near as possible to those in the current study were selected as starting sets in the search. To avoid ambiguities of the first type mentioned, a conventional search procedure was avoided in which four or six parameters are allowed to vary simultaneously. The search scheme we adopted is a six-parameter search in which only two parameters are allowed to vary at a time, the other four remaining fixed. The sequence of the variation in the search is as follows: (1) $V, W_{\text{vol.}}$; (2) r_0, r_0'; (3) a, a'; and (4) $V, W_{\text{vol.}}$, where the symbols for the parameters have the usual meaning. The searches were made by the optical-model search code JIB without a spin-orbit potential and with a local potential.[20]

1. ^{3}He Parameter Search

Cates recently measured the ^{3}He-Zr elastic scattering angular distribution at 30.9 MeV, from which a family of ^{3}He parameters was searched and successfully utilized in the DWBA analysis of the Zr(^{3}He, d) reactions.[21] The "average" parameter Set 1 with a real-well depth of $U_{^3\text{He}} = 151$ MeV from Cates's ^{3}He parameters was chosen as the start set for the ^{3}He parameter search. No meaningful search could be made with our 15-MeV ^{3}He elastic scattering data, because of the dominance of Coulomb scattering. When Cates's start set was directly compared with our 20-MeV data, the χ^2 per data point was 2.24. This reduced to 0.62

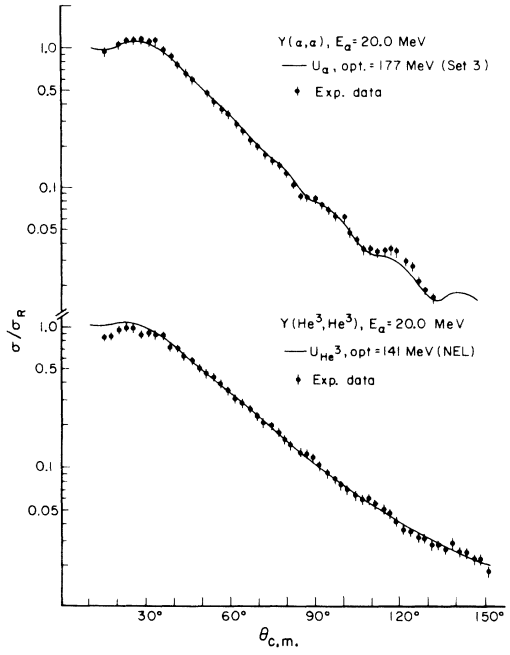

FIG. 3. The ratios of the measured α-Y and ^{3}He-Y elastic scattering cross sections to the Rutherford cross sections. The curves are the optical-model fits to the data. The α and ^{3}He potential sets, obtained in a six-parameter search, are tabulated in Table I.

when the final search was made. Cates's Set 1 and our final searched set (NEL set) are listed in Table I. The fit of the NEL set to the measured angular distribution at 20 MeV is shown in the lower portion of Fig. 3. Searches based on Cates's two deeper sets (Set 2 with $U = 172$ MeV and Set 3 with $U = 185$ MeV) were not made, because the simple picture of the ^{3}He-nucleus interaction potential gives a simple superposition of three nucleon-nucleus optical potentials, namely a real-well depth on the order of 150 MeV.

2. α Parameter Search

The three α parameter sets obtained from a four-parameter search by McFadden and Satchler for Zr at 24.7 MeV[22] were chosen as the start sets. The searched NEL sets are listed in Table I. The four-parameter search was also conducted and the results were nearly identical to the corresponding parts of the six-parameter results. All three sets were obtained in the α case so that detailed sensitivity checks of the effect of the α parameters on the (d, α) calculations could be made. The measured angular distribution is compared with NEL Set 3 in the upper half of Fig. 3. The data points were raised by 5% before the search was made. This renormalization of the data was carried out by normalizing the original data points to the essentially parameter-independent forward-angle scattering cross sections calculated by JIB.

B. ^{89}Y(^{3}He, α)^{88}Y Reaction

The extent to which standard DWBA methods can be reliably used for analysis of a direct (^{3}He, α) transition was extensively studied by Stock *et al.* for the Cr(^{3}He, α) reaction.[19] A dominant factor influencing the efficacy of the (^{3}He, α) reaction as a spectroscopic tool is the momentum matching condition. In the case of good momentum matching (that is, when the L gaps in the partial waves for the entrance and exit elastic channels are filled by the l values of the transitions) the angular distributions are l characteristic; and the local zero-range noncutoff DWBA calculations reproduce the measured angular distributions of the stronger transitions fairly well if proper potentials searched from the measured elastic scattering are used. In the mismatch case the conventional DWBA approximations successfully used for surface reactions such as (d, p) and (^{3}He, d) become less appropriate. The reaction is strongly influenced by the nuclear interior portion of the wave functions, so the standard method of using the best-fit elastic scattering parameters to generate distorted waves for the reaction analysis is not always justified in this case since the elastic scattering is not sensitive to contributions from the nuclear interior. Thus there exists an ambiguity associated with the selection of the proper combination of optical-model potentials both in the entrance and exit channels.

For the conventional DWBA treatment for (^{3}He, α)

TABLE I. Optical-model-potential parameters in standard notation used in the (d, α) and (^{3}He, α) DWBA analysis. NEL sets are the searched sets from the present work. χ^2 for ^{3}He-^{52}Cr and ^{3}He-Zr sets, and the α-Zr set were obtained from direct comparison with our measured ^{3}He-Y and α-Y elastic scattering angular distributions at 20 MeV.

			Real-well parameters					Imaginary-well parameters				
Channel	Set	Ref.	E (MeV)	U (MeV)	r_0 (F)	r_c (F)	a (F)	W_{vol} (MeV)	W_{surf} (MeV)	r'_0 (F)	a' (F)	χ^2 (per point)
d-^{90}Zr	Perey-Perey Set 2	33	15.0	98.1	1.127	1.127	0.848	...	14.87	1.394	0.655	...
^{3}He-Y	NEL	This work	20.0	141.6	1.235	1.4	0.692	22.2	...	1.536	0.795	0.62
^{3}He-^{52}Cr	Stock's modified set	19	19.5	142.4	1.362	1.4	0.65	12.67	...	1.755	0.781	0.93
^{3}He-Zr	Cates's Set 1	21	30.9	151.0	1.24	1.4	0.69	20.0	...	1.55	0.80	2.24
α-Y	NEL Set 1	This work	20.0	52.93	1.568	1.4	0.528	10.28	...	1.569	0.485	0.55
α-Y	NEL Set 2	This work	20.0	146.1	1.464	1.4	0.515	18.25	...	1.470	0.449	0.70
α-Y	NEL Set 3	This work	20.0	177.2	1.443	1.4	0.514	19.84	...	1.459	0.445	0.66
α-Zr	M-S Set 3	22	24.7	187.3	1.444	1.4	0.523	22.3	...	1.444	0.523	1.65
α-^{50}Ti	Stock's modified set	19	30.5	183.7	1.4	1.4	0.56	26.0	...	1.48	0.56	...

reactions to be valid, especially in the case of a momentum mismatch, Stock *et al.*[19] concluded that the potential for the outgoing α must be close to the sum of the potentials for the incident ^{3}He and the transferred neutron. Also the zero-range approximation in the DWBA is a poor one for a reaction which involves a large momentum transfer and momentum mismatch.[23] If there is such a mismatch, the results of the DWBA calculations will depend rather strongly on the cutoff radius,[18,19] but no clear criterion exists for the choice of a particular cutoff radius. Inclusion of the corrections of finite range of interaction and nonlocality of the potentials into the zero-range DWBA has the effect of reducing the contributions from the nuclear interior in a smooth way.[24,25] Hence, strong effects on the shape of the angular distributions are expected in the mismatch case when these corrections are treated properly in the DWBA analysis.

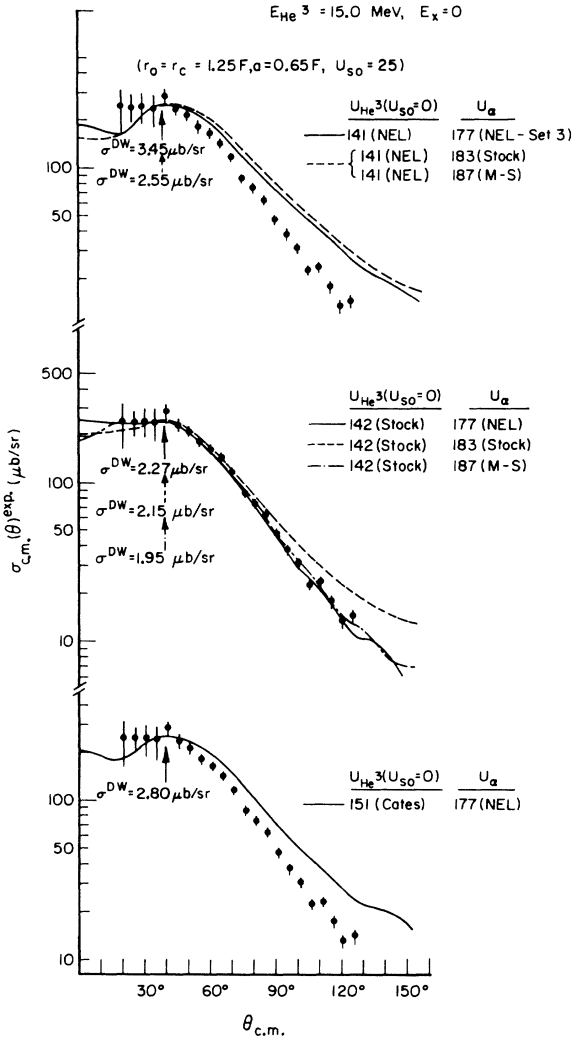

FIG. 4. Sensitivity checks of ^{3}He- and α-potential combinations for the ^{89}Y(^{3}He, α) DWBA analysis. The measured angular distribution for the ground-state transition is compared with $l_n = 4$ local zero-range DWBA predictions (curves) based on the three different α sets combined with fixed ^{3}He sets. The curves are normalized to the data at about 40° where the cross sections $(2s+1)\sigma^{DWUCK}/2(2j+1)$ are indicated. All potential sets are given in Table I.

Sensitivity of DWBA calculations to potential parameters and to corrections for nonlocality and finite-range effects will be checked in some detail in this section. All (^{3}He, α) calculations were made with the DWBA code DWUCK.[26] Both corrections may be conveniently entered as an option into DWUCK.

1. *Effects of Parameter Variations on DWBA Calculations*

(i) Optical-model potentials. All (^{3}He, α) transitions to the levels below 2-MeV excitation in ^{88}Y (except to the 1.7-MeV level) are known to proceed by $l_n = 4$ and $l_n = 1$ transfers.[8,9] Although parameter sensitivity of the calculations was studied for both $l_n = 1$ and 4 transfers, the results obtained for the $l_n = 4$ ground-state transition will be the only one discussed in detail here. The results for l_n transfers to other states lead to basically the same conclusions as do the ground-state transition results.

The L gaps in the partial waves for the ^{3}He and α channels for the Q values of interest are three or four angular momentum units. Thus it is expected that zero-range local calculations with proper optical-model potentials should be able to reproduce the measured angular distribution for the ground-state transition. The results of the zero-range local calculations based on various combinations of ^{3}He and α potentials, which are listed in Table I, are compared with the data for the ground-state transition in Fig. 4. The calculations are normalized to the data at about $\theta = 40°$, where the magnitudes of the cross sections calculated by DWUCK are indicated. The neutron bound-state wave function was generated from a Woods-Saxon (W-S) well with $r_0 = r_{0c} = 1.25$ F and $a = 0.65$ F. A Thomas spin-orbit term with a coefficient of $V_{so}^n = 25$ was also included. Following the separation energy prescription, the well depth U was searched by DWUCK to bind the neutron with the experimentally known separation energy.

The curves in the top portion of Fig. 4 show the effects of various α potentials combined with the same NEL ^{3}He set with $U_{^3He} = 141$ MeV. The solid curve illustrates the calculation based on the NEL α Set 3 with $U_\alpha = 177$ MeV and the dashed curve corresponds to the calculation based on the modi-

fied α set of Stock *et al.* with $U_\alpha = 183$ MeV.[19] This modified set was obtained through readjustment of the original potential parameters (which were searched from the measured α-particle ^{50}Ti elastic scattering angular distribution) by relaxing the requirement on the quality of the fit to the elastic scattering data while requiring the χ^2 for the ^{54}Cr-(^{3}He, α) reaction data fit to be improved. The calculation based on α Set 3 ($U_\alpha = 187$ MeV) by McFadden and Satchler (M-S α Set 3)[22] is also represented by the dashed curve since it is almost identical in shape to the calculation based on Stock's set. It is obvious that none of the calculations reproduce the data, especially the slope, and this is in disagreement with the prediction described earlier.

In the center portion of Fig. 4 the potential sensitivity check is repeated with different α sets combined with the same ^{3}He set which was the modified ^{3}He set obtained by Stock *et al.*[19] by the procedure described above. The broken curve is the calculation made with M-S α Set 3. Combinations of Stock's modified ^{3}He set with NEL α Set 3 and with M-S Set 3 lead to almost perfect fits to the data, while the combination with Stock's modified α set results in a misfit. This last potential combination is that which Fou and Zurmühle[8] successfully used in their analysis of the ^{89}Y(^{3}He, α) reaction at 18 MeV, and it was also used by Stock *et al.*[19] in their analysis of the ^{54}Cr(^{3}He, α) reaction at 19.5 MeV. Furthermore, this particular combination satisfies the potential criterion of Stock which was described earlier. Inclusion of the finite-range and nonlocality corrections has failed to improve the quality of the calculations to any noticeable degree.

The curve at the bottom of Fig. 4 represents the calculation based on Cates's ^{3}He set and NEL α Set 3. Comparison of all three solid curves in Fig. 4 indicates clearly that of the three ^{3}He sets tried only Stock's modified set forms an acceptable combination with NEL α Set 3 to reproduce the data.

(ii) Nonlocality and finite-range correction. The nonlocality correction was made with a radial correction factor in the local-energy approximation (LEA).[4] We used the standard range values of $\beta_n = 0.85$, $\beta_{^3\mathrm{He}} = 0.3$, and $\beta_\alpha = 0.2$ F used in Ref. 19. The finite-range correction was also made with the LEA correction factor. The form of the correction factor originally incorporated into DWUCK included higher-order corrections,[4,26] but it has a built-in defect in that it possesses a singularity at a radius around the surface when a large value of the range ($1.5 \leq R \leq 2.0$) prescribed for the (^{3}He, α) reaction and the best potential combination described earlier are used. This difficulty is resolved when the more frequently used first-order term[4]

$$\Lambda(r) = 1 - R^2 C_1 [U_\alpha(r) - U_{^3\mathrm{He}}(r) - U_n(r) - \epsilon] \qquad (1)$$

is used. Here the U's are the potentials for the ^{3}He, α, and the bound neutron. The energy required to separate a neutron from an α particle is given by $\epsilon = 20.6$ MeV, and C_1 is a constant involving the particle masses. Inserting the best potential combination (Stock's modified ^{3}He set and NEL α Set 3 in Table I), and $R = 1.5$ F, we find from the real part of (1) that the finite-range f.f. is enhanced uniformly by a factor of 2 or 3 over its zero-range counterpart. To remedy the incorrect asymptotic behavior of the over enhancement, Stock *et al.*[19] proposed to attenuate the real part of (1) by a factor of $(1 + C_1 \epsilon R^2)^{-1}$.

In Fig. 5 products of the "attenuated" finite-range and nonlocality correction factors are plotted as a function of radius. The solid curve represents this product for the $1g_{9/2}$ transfer, and the dashed curve is for the $2p_{1/2}$ transfer, both being attenuated by 0.373. The nonlocality correction for the bound state was not made for the extraction of spectroscopic information, since the accuracy of the LEA is known to be questionable in this case.[19,27] After the corrections were made in the radial wave functions, they were found to be reduced in the nuclear interior by 50 to 60% and enhanced in the surface region by approximately the same amount.

The calculations made with the inclusion of the corrections (dashed curve) and without (solid curve)

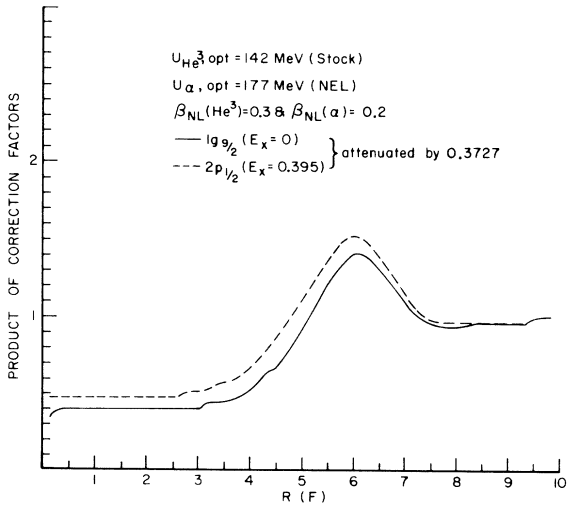

FIG. 5. The products of the LEA finite-range and nonlocality correction factors for the ^{89}Y(^{3}He, α) reaction. The finite-range correction is that of the first-order form of (2), attenuated by $(1 + C_1 \epsilon R^2)^{-1}$ to ensure the correct asymptotic behavior of the form factors.

are compared with the measured angular distributions for the ground state and 0.394-MeV transitions in Fig. 6. The broken curves represent the local zero-range calculations based on the potential combination of the NEL ^{3}He set and α Set 3, previously tried for the $l_n = 4$ calculation only. It is demonstrated at the bottom of the figure that this combination of potentials fails to reproduce the slope of the measured $l_n = 1$ angular distribution also. The $l_n = 4$ calculations are normalized to the data points around 40° as before, and the $l_n = 1$ calculations are normalized to the data around 65°, where the calculated cross sections are indicated. As anticipated, no marked change is seen between the calculations with and without the corrections for the $l_n = 4$ ground-state transition. The $l_n = 1$ zero-range calculation exhibits a strong oscillating pattern which the measured angular distribution does not possess. The nonlocal finite-range calculation succeeds in smoothing out the fluctuations, thereby fitting the data better. This improvement in the calculation due to the corrections is expected for $l_n = 1$ transitions because of the momentum mismatch condition mentioned earlier.

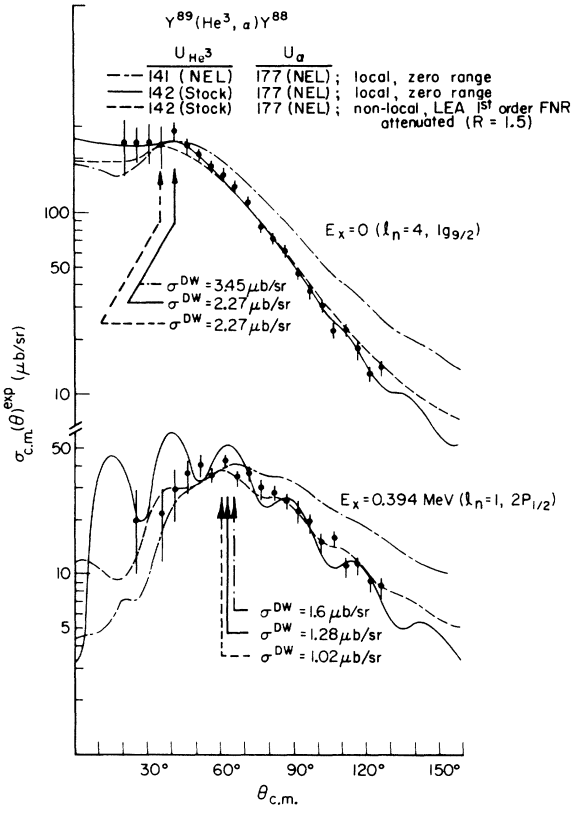

FIG. 6. Comparison between the local zero-range and nonlocal finite-range DWBA calculations for the $l_n = 4$ transition to the ground state of ^{88}Y in the top of the figure, and the $l_n = 1$ transition to the 0.394-MeV state in the bottom. The nonlocal finite-range calculations are based on the corrections shown in Fig. 5. The potential combinations used in the calculations are specified in the figure.

The measured angular distributions for the remaining six transitions obtained are shown in Fig. 7, where they are compared with the local zero-range (solid curve), and nonlocal finite-range (dashed curve) calculations. These calculations were made with the potential combination of Stock's ^{3}He set and NEL α Set 3. The dependence of the bound-state wave function and the distorted wave in the α channel on the Q value has been correctly treated.

2. *Spectroscopic Factors and Normalization*

Spectroscopic factors were extracted by comparing the measured cross sections with both the local zero-range and the nonlocal finite-range DWBA calculations. The relationship used to extract the spectroscopic factors for neutron pickup with angular momentum transfer l, j is given as[26]

$$\left(\frac{d\sigma}{d\Omega}\right)_{l,j}^{\exp} = CS_{l,j}\left[\frac{2s+1}{2}\,\frac{\sigma_{l,j}(\theta)^{\mathrm{DW}}}{2j+1}\right]. \tag{2}$$

Here $\sigma_{l,j}(\theta)^{\mathrm{DW}}$ is the reduced cross section calculated by DWUCK, and $S_{l,j}$ is the spectroscopic factor. The (^{3}He, α) reaction populates both $T_<$ and $T_>$ states, the latter being the analog of $T_>$ states in the target minus proton nucleus. The corresponding spectroscopic factors, $S_<$ and $S_>$, satisfy the well-known sum rules.[28] The theoretical range of the value of the normalization constant C was given by Bassel as $18 \leq C \leq 25$.[29] Several empirical values for C which were determined with the use of the sum-rule limit on $S_<$ were found to fall within these limits.[8,9,19] Applying this sum rule to the $g_{9/2}$ transfers observed in the present reaction, an empirical value of $C = 25$ was obtained when the local zero-range calculations were used. Based on this value, the spectroscopic factors for the eight transitions have been extracted with the use of both the local zero-range and the nonlocal finite-range calculations. The extracted factors are compared with the predictions of the sum-rule limits and are summarized in Table II. The $\sigma_{l,j}(\theta)^{\mathrm{DW}}$ were calculated with the parameters listed in Table III. With $C = 25$ the extracted spectroscopic factors from the current study are in better agreement with those determined in Ref. 8 (which are also based on $C = 25$) than those in Ref. 9 (which are based on $C = 27$). Only local zero-range calculations were used in Refs. 8 and 9.

The errors assigned to the spectroscopic factors in Table II are those associated with the am-

TABLE II. Summary of the (^{3}He, α) spectroscopic factors obtained from the present work. Relative spectroscopic factors $S_{rel.}$ in columns 5 and 7 were obtained from direct comparison between the measured angular distributions and the local zero-range and nonlocal finite-range DWBA cross sections calculated with DWUCK based on the parameters listed in Table III. The absolute spectroscopic factors $S_{abs.}$ in columns 6 and 8 were extracted on the basis of $C = 25$. This normalization constant value was obtained by normalizing the sum of the ground state and 0.232-MeV state spectroscopic factors to 10, which is the sum-rule limit as shown in column 4.

E^* (MeV)	l_n	Probable $(nlj)_n$	Sum-rule limit $2j_n+1$	Local and Z.R. $S_{rel.}$	Local and Z.R. $S_{abs.}$	N.L. and F.R. $S_{rel.}$	N.L. and F.R. $S_{abs.}$
0	4	$1g_{9/2}$	10	110 ± 13	4.4 ± 0.3 [a]	110 ± 13	4.4 ± 0.3
0.232	4	$1g_{9/2}$		141 ± 9	5.6 ± 0.3 [a]	136 ± 8	5.5 ± 0.3
0.394	1	$2p_{1/2}$	2	29.7 ± 4	1.2 ± 0.1	37.3 ± 5	1.5 ± 0.2
0.767	1	$2p_{1/2}$		15.4 ± 2	0.62 ± 0.05	17.2 ± 2	0.7 ± 0.1
1.220	1	$2p_{3/2}$	4	24.0 ± 3	0.96 ± 0.1	25.3 ± 3	1.0 ± 0.1
1.279	1	$2p_{3/2}$		39.3 ± 2	1.6 ± 0.1	41.0 ± 3	1.6 ± 0.1
1.560 + 1.596	1	$2p_{3/2}$		46.1 ± 3	1.9 ± 0.1	48.6 ± 3	1.9 ± 0.1
1.705	3	$1f_{5/2}$	6	65.2 ± 4	2.6 ± 0.2	68.7 ± 10	2.7 ± 0.5

[a] Normalized value.

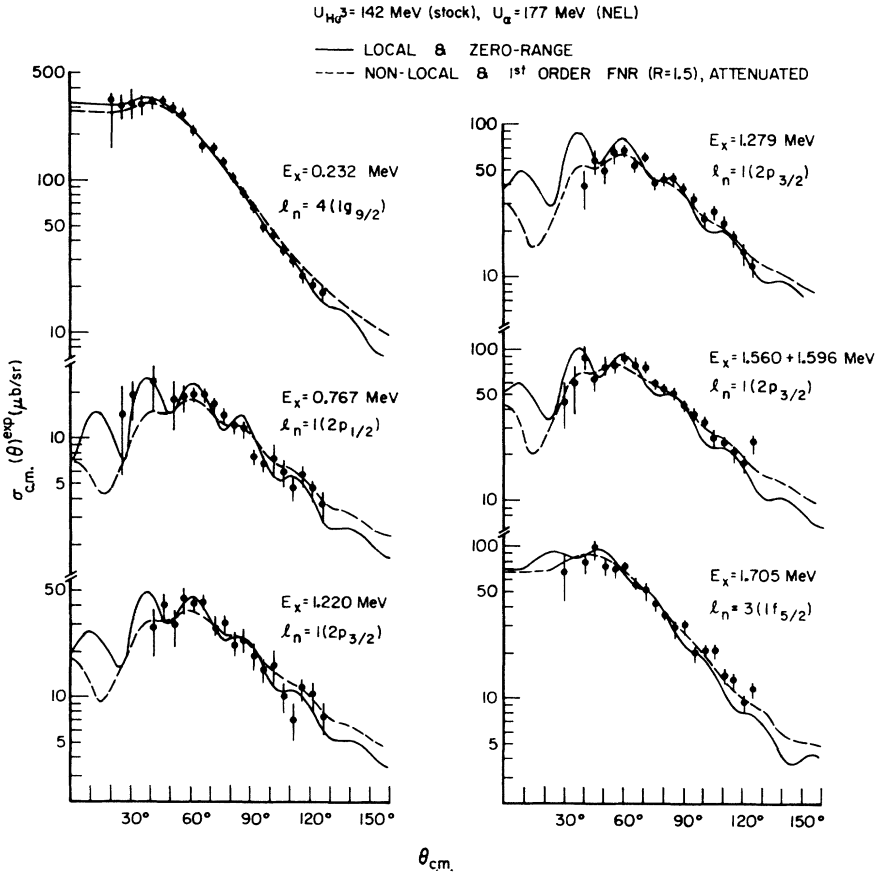

FIG. 7. The six remaining measured (^{3}He, α) angular distributions compared with local zero-range and nonlocal finite-range DWBA calculations. All calculations were made on the basis of the correct Q values.

biguities in fitting the curves to the data at the angles where the cross sections are compared. The more serious errors to be considered are not included in the above errors. They are due to variations in the calculated cross-section magnitudes when the parameters other than those listed in Table III are used in the calculations. Since this aspect of the analysis has been studied in detail in previous works[19, 8, 9] this type of sensitivity check has not been made in the present work.

3. j_n Assignments

It has been reported that j dependence has been recognized in certain (^{3}He, α) reactions for $l_n = 1$ and $l_n = 3$ transfers.[19] A search for j dependence in our measured angular distributions was not practical for the most part because of relatively large random errors assigned to much of the data, although j dependence was recognized for the $l_n = 1$ transfers in the local zero-range calculations. From shell-model considerations and with the aid of the sum-rule limits, some j_n assignments can be inferred with certainty. Assuming that the neutron orbits in ^{89}Y are closed for 50 neutrons, the assignment of $1g_{9/2}$ to the $l_n = 4$ transitions to the ground state and the 0.232-MeV state appears unique. The sum of the $g_{9/2}$ spectroscopic factors extracted with the nonlocal finite-range calculations was 9.9 compared with the sum-rule limit of 10. This demonstrates that (^{3}He, α) transitions associated with the momentum-matching condition are insensitive to details of the calculations once the proper potential combination is used. Assignment of $j_n = \frac{1}{2}$ to the $l_n = 1$ transitions to the 0.394- and 0.767-MeV states is plausible judging from the locations of single-particle states for this mass region. This assignment is also supported by the observation that the sums of the $p_{1/2}$ spectroscopic factors for these two levels are 1.82 for the zero-range calculations and 2.2 for the finite-range calculations. These two values agree with the sum-rule limit of 2 for the total $p_{1/2}$ strength to within ±10%.

l_n transfers to the closely spaced doublet at 1.2 MeV and the unresolved doublet at 1.57 MeV appear to be associated with $j_n = \frac{3}{2}$ transfers, since the total strength available for $p_{1/2}$ transfers has already been exhausted. The sum of the $p_{3/2}$ spectroscopic factors for these levels is about 4.5 which exceeds the sum-rule limit of 4 by about 12%. Identification of an $l_n = 3$ transfer to a level at 1.7 MeV as an $f_{5/2}$ pickup is considered reliable from the shell-model picture. The measured spectroscopic factor is 2.6 which is far less than the predicted limit of 6, indicating that the $f_{5/2}$ single-particle strength is highly fragmented. Since no prominent levels above 1.7 MeV were populated in the (^{3}He, α) reaction, the remainder of the $f_{5/2}$ strength went undetected. A simple weak-coupling picture then appears no longer valid at such high excitation energies, since each neutron single-particle strength is expected to be split between just two levels as the ground state J^π of ^{89}Y is known to be $\frac{1}{2}^-$. The j_n assignments made in the present work are in agreement with those proposed in Refs. 8 and 9, and they are listed in Table II.

C. ^{90}Zr(d, α)^{88}Y Reaction

1. DWBA Formalism of Direct (d, α) Transition with Inclusion of the Finite-Range Correction

The DWBA theory of a two-nucleon transfer reaction which we follow for our (d, α) analysis is basically the zero-range formalism of Glendenning[2] except for the two-nucleon form factor which is based on the oscillator-expansion technique of Drisko and Rybicki.[6] The finite-range effects are handled by the formalism of Chant and Mangelson.[5] The zero-range DWBA treatment of two-nucleon transfer reactions leads to a differential cross section which is proportional to an incoherent sum over L, S, and J of the transferred pair when the spin-orbit coupling is not included in the distorted-wave channels:

TABLE III. Parameters used in DWUCK for calculating the reduced cross sections for extraction of the l_n transfers and spectroscopic factors tabulated in Table II. Both α and ^{3}He potential sets are given in Table I.

Optical-model potentials:	$V_{^3\mathrm{He}}$ = Stock's modified Set (Ref. 19) with $U_{^3\mathrm{He}} = 142$ MeV V_α = NEL Set 3 with $U_\alpha = 177$ MeV
Form-factor parameters:	$r_0 = r_c = 1.25$ F, $a = 0.65$ F B.E. = S.E. + E_x, $U_{so}^n = 25$
Nonlocality parameters: (LEA correction)	$\beta_{^3\mathrm{He}} = 0.3$ F, $\beta_\alpha = 0.2$ F, $\beta_n = 0.0$ F
Finite-range correction: (LEA first order, attenuated)	$R = 1.5$ F

$$\left(\frac{d\sigma}{d\Omega}\right)^{\text{Z.R.}} \propto \sum \left| \int \chi^{(-)*}(\vec{K}_\alpha, \vec{R}) F_{LSJ}(R) \times Y_L^M(\hat{R}) \chi^{(+)}\left(\vec{K}_d, \frac{A-2}{A}\vec{R}\right) d\vec{R} \right|^2 . \tag{3}$$

Here the χ's are the distorted waves for the incident deuteron and outgoing α particle with relative momenta $\vec{K}_d$ and $\vec{K}_\alpha$, respectively. They are generated by the optical-model potentials. $F_{LSJ}(R)$ is the two-nucleon form factor which is obtained from a coherent sum over all two-particle configurations, γ, present in the nuclear wave functions, and is expressed as[1]

$$F_{LSJ}(R) = \sum_\gamma \beta_{LSJ}^\gamma f_L^\gamma(R) . \tag{4}$$

Here β_{LSJ}^γ is the spectroscopic amplitude[2] for the configuration γ. The function $f_L^\gamma(R)$ is the f.f. for the pure configuration γ, and is, in essence, the radial wave function for the center-of-mass motion of the pair in the configuration γ coupled to L. R is the c.m. coordinate of the pair relative to the residual nucleus of mass $A-2$. The explicit form of $f_L^\gamma(R)$ depends on the method with which the f.f. are obtained. In the oscillator-expansion representation $f_L^\gamma(R)$ is reduced to[2, 5, 6]

$$f_L^\gamma(R) = \sum_N A_N \phi_M^{NL}(2\nu R^2) , \tag{5}$$

where

$$A_N = \sum_{\substack{n_1, n_2 \\ n}} C_{n_1} C_{n_2} \Omega_n \langle n0, NL : L \,|\, n_1 l_1, n_2 l_2 : L \rangle . \tag{6}$$

C_{n_i} are the coefficients for the expansion of finite-well single-particle wave functions into a series of harmonic-oscillator functions. $\langle \,|\, \rangle$ are the Moshinsky-Brody brackets which appear when the products of the oscillator wave functions with quantum numbers n_i and l_i are transformed into products of the relative wave functions with n, l, and the c.m. wave functions $\phi_M^{NL}(2\nu R^2)$ with N and L, in which ν is the oscillator size parameter.

The relative wave function of the pair has to overlap with that part of the α particle and this overlap is Ω_n in (6). This overlap is obtained in a closed form when a Gaussian form is assumed for the α particle, expressed as

$$\Phi_\alpha = N e^{-\eta^2 \sum \vec{r}_{ij}^{\,2}} \tag{7}$$

$$= \phi^{10}(4\eta^2 \vec{r}_d^{\,2}) \phi^{10}(4\eta^2 \vec{r}^{\,2}) \phi^{10}(8\eta^2 \vec{\rho}^{\,2}) , \tag{8}$$

where η is the α size parameter, and $\vec{r}_d$, $\vec{r}$, and $\vec{\rho}$ are the relative coordinates of the incoming deuteron, the pair, and the outgoing α particle, respectively.

The transition amplitude of (3) is based on the zero-range assumption in which the product of the interaction as a function of ρ and that part of the α wave function also depending on ρ is replaced by a δ function. The form of Ω_n is modified when a Gaussian form is also assumed for the nucleon-nucleon interaction,[5]

$$V_{ij} = V_0 e^{-\mu^2 r_{ij}^{\,2}} \tag{9}$$

$$\simeq 4 V_0 \exp[-\mu^2(\rho^2 + \tfrac{1}{4}r^2 + \tfrac{1}{4}r_d^{\,2})] , \tag{10}$$

where μ is the range of the interaction. $\hat{\Omega}_n$, the overlap integral over the relative coordinates $\vec{r}$, then includes that part of V_{ij} which also depends on r.

The zero-range transition amplitude in (3) is then modified by an exponential correction factor which is, to first order,[5] proportional to

$$\exp[(C_2/4\epsilon^2)(V_d - V_\alpha + V_x + S_x)] . \tag{11}$$

Here C_2 is a constant involving the particle masses, V_d and V_α are the optical potentials, and V_x is the binding potential for the pair. S_x is the energy required to break up the α particle into a deuteron plus the pair. The "total range" ϵ is related to the ranges η and μ by

$$\epsilon^2 = \mu^2 + 4\eta^2 . \tag{12}$$

The "zero-range" f.f., $F_{LSJ}(R)$, in (3) is now replaced by the "finite-range" f.f. which is based on $\hat{\Omega}_n$ instead of Ω_n when the residual interaction is taken into consideration. The overlap between the incident deuteron wave function and the relevant part of the α wave function in (8), Ω_d, which acts only as an over-all normalization factor, also includes the corresponding part of the interaction V_{ij} of (10).

2. *DWBA Calculations*

The differential cross section for (d, α) can be written as[26, 30]

$$\frac{d\sigma(\theta)}{d\Omega} = D_0^2(d, \alpha) \left[\frac{2S+1}{2} \frac{\sigma(\theta)^{\text{DW}}}{2J+1}\right] \tag{13}$$

with

$$D_0^2 \propto \tfrac{1}{3} \Omega_d^2 V_0^2 , \quad \left(\frac{2s_\alpha + 1}{2s_d + 1} = \frac{1}{3}\right) . \tag{14}$$

$\sigma^{\text{DW}}(\theta)$ is the reduced cross section calculated by DWUCK. DWUCK calculates the differential cross section given in (3) for the zero-range case and then modifies the zero-range transition amplitude in (3) by the exponential correction factor of (11) to obtain the finite-range cross section. The absolute cross-section normalization is $D_0^2(d, \alpha)$ which is proportional to the product of Ω_d^2 and V_0^2, the strength of the interaction in (9).

In this work the two-nucleon f.f. defined in (5) and (6) were generated separately by the code MIFF[6] of Drisko and Rybicki[31] and were read into DWUCK externally. The $f_L^\gamma(R)$'s are not the complete two-nucleon f.f. which are required to be entered into the transition amplitudes when there is more than one two-particle configuration contributing to a transition. The $f_L^\gamma(R)$ should be weighted by the spectroscopic amplitudes β_{LSJ}^γ and the weighted "partial form factors" be summed over all the pair configurations γ in order to obtain the complete two-nucleon f.f. $F_{LSJ}(R)$ as given in (4). However, β_{LSJ}^γ for the ^{90}Zr$(d, \alpha)^{88}$Y reaction cannot be furnished at present as the complete initial and final wave functions appropriate to this reaction have not been calculated as of yet. Thus, f_L^γ for each L were obtained for pure two-particle configurations which are expected to contribute predominantly to transfers of interest. The f.f.

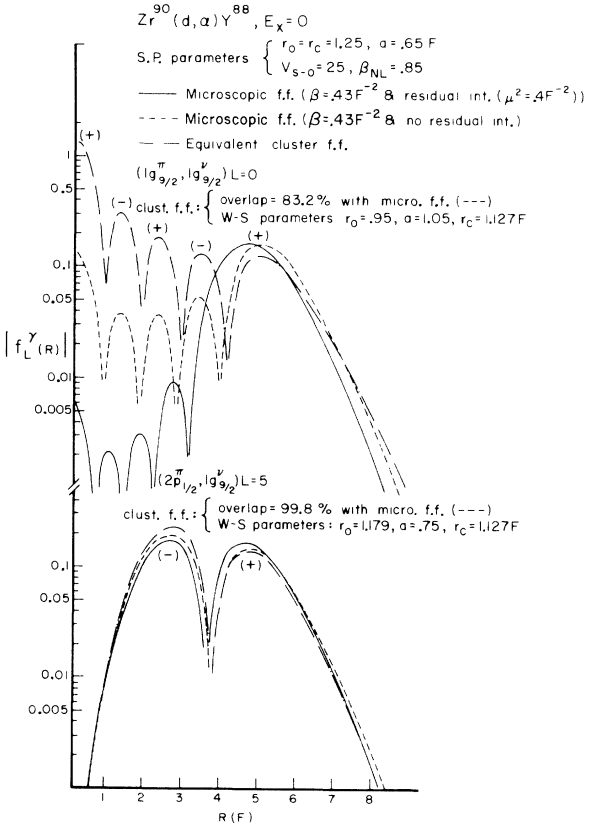

FIG. 8. Comparison of two-nucleon form factors (f.f.) with (solid curves) and without (dashed curves) the inclusion of the residual interaction and cluster f.f. (broken curve) equivalent to the latter f.f. The curves in the upper half represent the f.f. constructed from the $(1g_{9/2})^2_{L=0}$ pure configuration and those on the lower half represent the f.f. from the $(2p^\pi_{1/2}, 1g^\nu_{9/2})_{L=5}$ pure configuration. Note the drastic reduction of the $(1g_{9/2})^2_{L=0}$ finite-range f.f. in the nuclear interior.

were normalized to 1 before being read into DWUCK. The effects of differing pure configurations on both f.f. and the cross sections will be discussed later.

(i) Two-nucleon form factors and relative angular distributions. From shell-model considerations, $1g_{9/2}$ and $2p_{1/2}$ orbits were chosen for the neutron single-particle wave functions (s.p.w.f.), and $1g_{9/2}$ and $2p$-$1f_{5/2}$ orbits were chosen for the proton s.p.w.f. Finite-well s.p.w.f. were generated from a Woods-Saxon well with the standard single-nucleon geometries of $r_0 = r_C = 1.25$ and $a = 0.65$ F. A spin-orbit strength of 25 times the Thomas term was also used. No unique prescriptions have been given as to the choice of the proper single-particle binding energies in the (d, α) case. Deahnick and Park adopted the "sequential pickup mode" for this purpose in their analysis of the ^{68}Zn(d, α) reaction.[1] The proton and neutron separation energies $E_s(p)$ and $E_s(n)$ associated with the two possible pickup modes are averaged; and they satisfy the energy balance $\langle E_s(p)\rangle_{\rm av} + \langle E_s(n)\rangle_{\rm av} = E_s(d) + 2.235$ MeV, where $E_s(d)$ is the separation energy of the deuteron from the core. For transitions to excited states, half the excitation energy is added to each single-particle binding energy. Following this prescription, $\langle E_s(p)\rangle_{\rm av} = 11.74$ MeV and $\langle E_s(n)\rangle_{\rm av} = 8.12$ MeV were used for transitions to low-lying states in ^{88}Y for the present ^{90}Zr(d, α) reaction.

In the following discussion, only the results based on an $L = 0$ transfer to the 0.394-MeV state and an $L = 5$ transfer to the 0.232-MeV state will be examined in detail, since unique J^π assignments for these levels have been previously made[32] and our measured (d, α) angular distributions show strong structure characteristic of $L = 0$ and $L = 5$ transfers, respectively.

(a) Two-nucleon f.f. with and without residual interaction and cluster f.f. Two-nucleon "microscopic" f.f. were calculated by MIFF with and without inclusion of the residual Gaussian interaction V_{ij} of (9). The "finite-range" and "zero-range" f.f. generated from $\hat{\Omega}_n$ and Ω_n are represented by solid and dashed curves in Fig. 8. The curves in the upper half of this figure are the f.f. constructed from the $(1g_{9/2})^2_{L=0}$ configuration, and the ones in the lower half are those from the $(2p^\pi_{1/2}, 1g^\nu_{9/2})_{L=5}$ configuration. The MIFF parameter $\beta \equiv 8\eta^2 \simeq 0.43$ F^{-2} based on the α size parameter[2] $\eta = 0.233$ F^{-1} was used throughout the MIFF f.f. calculations. The size parameter of the residual interaction, μ, is less well known. We used $\mu^2 = 0.4$ F^{-2} suggested in Ref. 5.

It is interesting to observe that while there is a marked difference in both the shape and magnitude of the two f.f. for the $(1g_{9/2})^2_{L=0}$ configuration, no

significant changes are observed between them for the case of the $(2p^{\pi}_{1/2}, 1g^{\nu}_{9/2})_{L=5}$ configuration. The finite-range f.f. is reduced by an order of magnitude inside the nucleus while a uniform reduction of about 50% is observed in the tail for the $(1g_{9/2})^2_{L=0}$ configuration.

The broken curves in Fig. 8 represent "equivalent cluster" f.f. They are generated under the assumption that a deuteron cluster is bound by the deuteron separation energy $E_s(d)$ in a Woods-Saxon well. The well geometries are searched by MIFF so that the resulting Woods-Saxon cluster f.f. has maximum overlap with the zero-range f.f., $f^{\gamma}_{L}(R)$. In the figure the $L=0$ cluster f.f. has a very poor (83%) maximum overlap with the corresponding zero-range microscopic f.f. with the searched well geometries of $r_0=0.95$ and $a=1.05$ F ($r_c=1.127$ F, fixed). The overlap of the $L=5$ cluster f.f. with the corresponding microscopic f.f. is excellent. The inability of the cluster f.f. to properly simulate the corresponding microscopic f.f. in the cases where the "angular momentum balance," $L \simeq l_p + l_n$, is far from satisfied has also been encountered in the past.[1] This difficulty may exist in part as a consequence of the large difference in the centrifugal potential barriers seen by single particles and the deuteron cluster.

The effect on the angular distribution of this poor representation of the $(1g_{9/2})^2_{L=0}$ microscopic f.f. by the equivalent cluster f.f. is pronounced as is clearly demonstrated in Fig. 9. The dashed curve represents the nonlocal finite-range calculation based on the zero-range microscopic f.f. and the broken curve represents the calculation based on the equivalent cluster f.f. shown in Fig. 8. While the data for the 0.232-MeV state is well reproduced by either $L=5$ calculation, the $L=0$ cluster calculation does not correctly predict the details of the structure of the data.

In Fig. 10 the results of the calculations based on the microscopic f.f. shown in Fig. 8 are compared with the measured $L=0$ and $L=5$ angular distributions. The $L=0$ curves are normalized to the data at about 40° and the $L=5$ curves at about

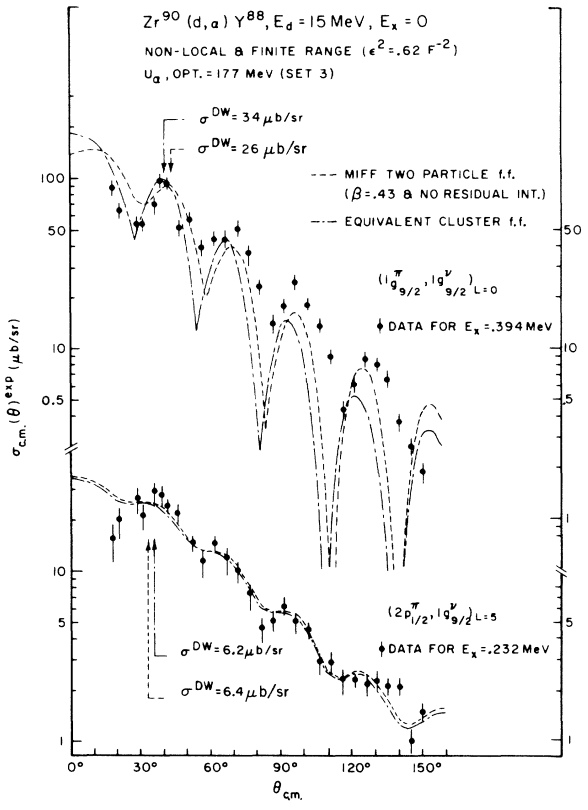

FIG. 9. Comparison of the effect of the zero-range microscopic f.f. and the equivalent cluster f.f. shown in Fig. 8 on the theoretical cross sections. The calculations for the $(1g_{9/2})^2_{L=0}$ transition to the 0.394-MeV state are normalized to the data at about 40° and those for the $(2p^{\pi}_{1/2}, 1g^{\nu}_{9/2})_{L=5}$ transition to the 0.232 state at about 35°.

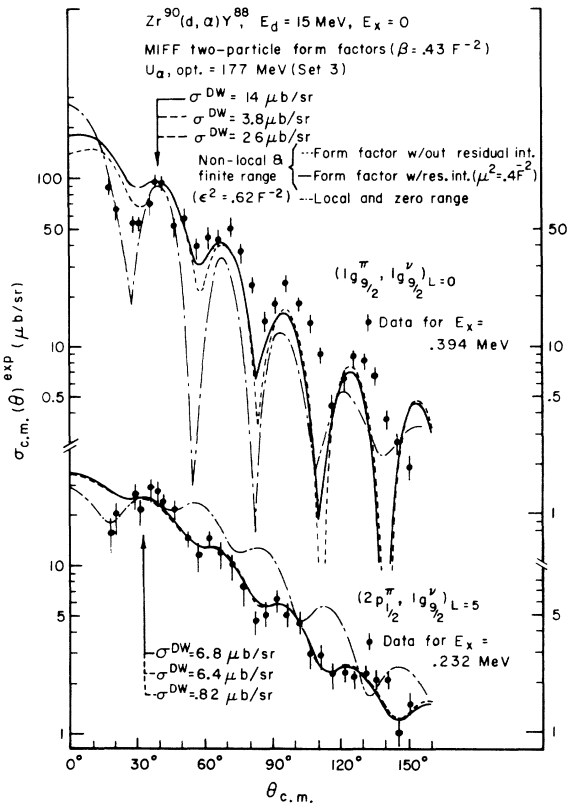

FIG. 10. Comparison between local zero-range and nonlocal finite-range DWBA calculations. The f.f. are the microscopic f.f. with and without the inclusion of the residual interaction shown in Fig. 8. The finite-range correction was made with the first-order correction of Chant and Mangelson. The nonlocality correction was made with the LEA correction including higher-order terms.

35°. The finite-range correction employed is that of (11), and the nonlocality correction is the LEA correction[4] with $\beta_{NL}^{d}=0.54$ and $\beta_{NL}^{\alpha}=0.2$ F.[26] The range parameter $\epsilon^2=0.62$ F^{-2} was obtained from (12). The α optical-model potential is NEL Set 3 listed in Table I with $U_\alpha=177$ MeV. The choice of this particular set over others will be discussed in detail in a later section. The deuteron potential is that of Perey[33] with $U_d=98$ MeV and is also listed in Table I. The solid curves in Fig. 10 correspond to the nonlocal finite-range calculations with the finite-range f.f. and the dashed ones are for the calculations using the zero-range f.f. The broken curves are for the local zero-range calculations with the zero-range f.f.

The local zero-range $L=0$ calculation predicts the locations of the stripping peaks of the data up to about 100° as accurately as the nonlocal finite-range calculations except that the slope of the former is too steep to reproduce the slope of the data. The zero-range $L=5$ calculation, however, completely fails to fit the over-all structure of the data. The principal effect of the inclusion of the residual interaction in the $(1g_{9/2})^2_{L=0}$ f.f. appears to be further smoothing out of the overemphasized sharp structure possessed by the zero-range calculation. The magnitude of the cross section based on the finite-range f.f. drops by a factor of about 2 compared with that based on the zero-range f.f.; this is well accounted for by a uniform reduction of the finite-range f.f. relative to the zero-range f.f. in the important tail section, illustrated in Fig. 8. The shapes of the two types of nonlocal finite-range calculations for the $(2p_{1/2}^{\pi}, 1g_{9/2}^{\nu})_{L=5}$ configuration are almost indistinguishable, which is shown in the lower portion of Fig. 10. Both reproduce the data very well over most of the angular range under investigation. Furthermore, the magnitudes of the calculated cross sections are in good agreement with each other, as is expected from the near identity of the corresponding f.f. in Fig. 8.

It should be noted that the magnitudes of the nonlocal finite-range calculations for the $L=0$ and $L=5$ transfers are larger than those of the zero-range counterpart by a factor of as much as 8. This enhancement is due to the fact that the products of the finite-range and nonlocality correction factors are greater than 1 by several magnitudes at the nuclear surface as demonstrated in Fig. 13.

(b) Configuration effects. So far the $L=0$ calculations have been limited to the $(1g_{9/2})^2_{L=0}$ configuration. The two-particle components in the initial- and final-state wave functions which contribute to $L=$ even transitions to $J^\pi=(\text{odd})^+$ low-lying levels are most likely to consist of admixed configurations of $(1g_{9/2})^2$ and $(2p_{1/2})^2$. Therefore it appears necessary to investigate to what extent the calculation for a certain transition is configuration dependent.

In the upper half of Fig. 11 the normalized two-nucleon microscopic f.f. generated from the $(2p_{1/2})^2_{L=0}$ configuration are compared with those generated from the $(1g_{9/2})^2_{L=0}$ configuration. The calculations for the $(2p_{1/2})^2_{L=0}$ configuration with and without the residual interaction are shown by the dashed and broken curves. Unlike the case of the $(1g_{9/2})^2_{L=0}$ configuration, the effect of the inclusion of the interaction does not cause a reduction in the nuclear interior. In the lower half of this figure the results of the configuration effect for the $L=5$ transfer are summarized. The f.f. generated from the $(1f_{5/2}^{\pi}, 1g_{9/2}^{\nu})$ configuration are compared with the previously examined finite-range f.f. generated from the $(2p_{1/2}^{\pi}, 1g_{9/2}^{\nu})$ configuration. A considerable reduction in the nuclear interior is observed when the residual interaction is included in the calculation. The condition for

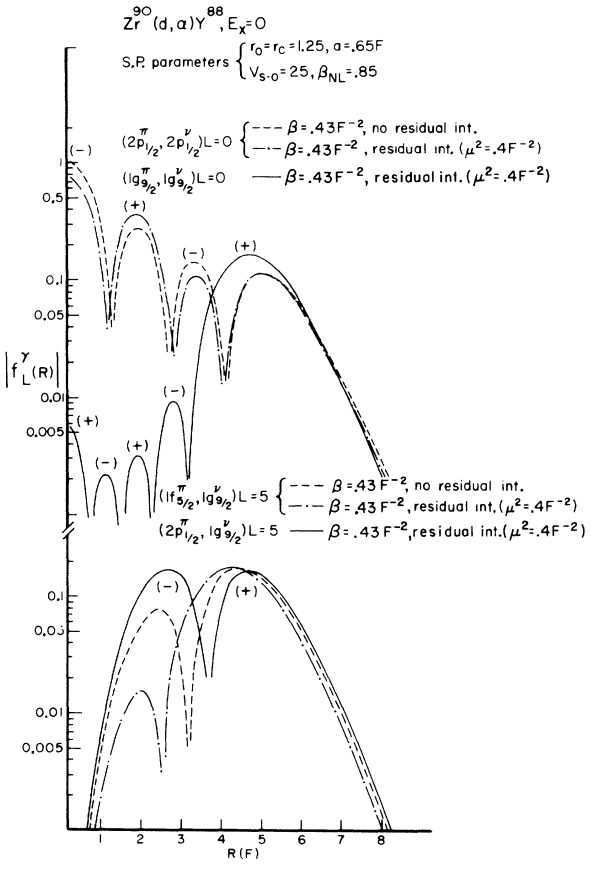

FIG. 11. The configuration dependence of the two-nucleon f.f. In the upper half the previously studied $(1g_{9/2})^2_{L=0}$ finite-range f.f. is compared with the $(2p_{1/2})^2_{L=0}$ f.f. In the lower half the previously investigated $(2p_{1/2}^{\pi}, 1g_{9/2}^{\nu})_{L=5}$ finite-range f.f. is compared with the $(1f_{5/2}^{\pi}, 1g_{9/2}^{\nu})_{L=5}$ f.f.

the angular momentum balance, considered previously in conjunction with the equivalent cluster f.f. search, appears to also be in effect in this case. The momentum balance condition, $l_p + l_n = L$, is far from being satisfied for the configurations where the finite-range f.f. are drastically reduced in the nuclear interior.

The effects of the different configurations on the cross sections are shown in Fig. 12. The nonlocal finite-range calculations based on the $(1g_{9/2})^2_{L=0}$ and $(2p_{1/2})^2_{L=0}$ finite-range f.f. shown in Fig. 11 are compared with the data in the upper half of Fig. 12. The comparable cross-section magnitudes are considered a consequence of the similarity of the tails of the corresponding f.f. The difference in the number of nodes between the two f.f., however, may well be responsible for the relative shifts in the locations of the stripping peaks of the angular distributions. The $L=5$ calculations compared with the data in the lower half of this figure indicate that the large difference in both the shape and magnitude in the nuclear interior between the $(2p^{\pi}_{1/2}, 1g^{\nu}_{9/2})_{L=5}$ and $(1f^{\pi}_{5/2}, 1g^{\nu}_{9/2})_{L=5}$ f.f. has little effect on the shape of the nonlocal finite-range cross sections. The observed insensitivity of the shape of the $L=5$ cross sections to the variations of configurations belonging to the same oscillator shell[1,2] permits the reliable extraction of $L=5$ transfers without detailed knowledge of the pertinent nuclear wave functions.

(c) Comparison between LEA cluster and two-nucleon finite-range corrections. The applicability of the LEA cluster correction formalism has been examined for the ^{90}Zr(d, α) reaction by comparing the LEA results with the calculations based on the two-nucleon finite-range correction formalism of Chant and Mangelson.[5] Figure 13 compares these two finite-range correction factors, multiplied by the same LEA nonlocality correction factors for the $(1g_{9/2})^2_{L=0}$ configuration. The solid curve corresponds to the two-nucleon correction factor of (11) with $\epsilon^2 = 0.62$ F^{-2}, and the dashed curve is that of the LEA cluster correction of (2) with the range of $R = 0.4$ F. This LEA range value has been determined empirically and used successfully by Daehnick and Park in their analysis of (d, α) reactions on even Zn isotopes.[1] Both curves are based on the same optical potentials. Although both correction factors peak at approximately the same radius, the extent of the enhancement differs significantly for the two; and this is expected to

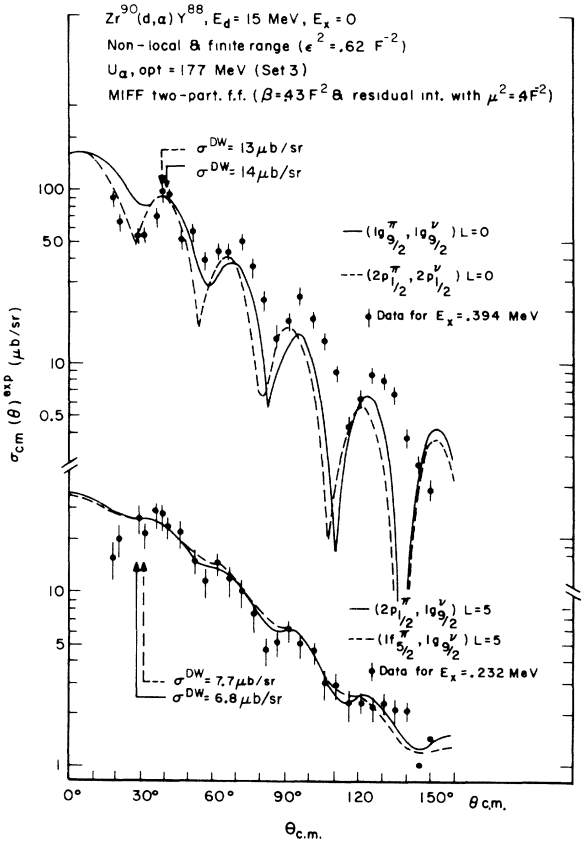

FIG. 12. Effect of configurations on the cross sections. The calculations are based on the finite-range f.f. shown in Fig. 11.

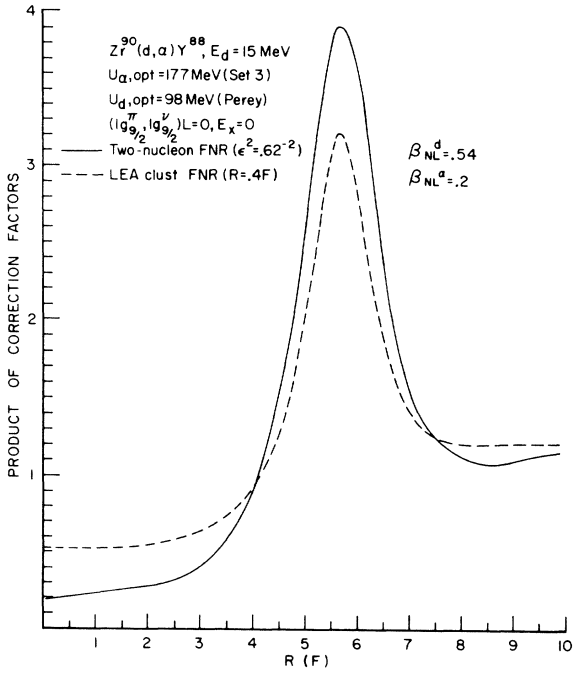

FIG. 13. Comparison of the products of the nonlocality and finite-range correction factors based on the two-nucleon formalism of Chant and Mangelson (14), and on the LEA cluster formalism (2).

measurably affect the magnitudes of the corresponding cross sections.

In Fig. 14 the cross sections based on the two-nucleon finite-range correction and on the LEA correction of Fig. 13 are compared with the data for the $(1g_{9/2})^2_{L=0}$ transition pictured in the upper half of the figure. The enhancement of the former over the latter is as expected; however, the latter calculation does not reproduce the locations of the stripping peaks of the measured angular distributions. The disagreement between the LEA calculation and the measured angular distribution is far more evident for the $L=5$ case as demonstrated in the lower half of Fig. 14.

(ii) Selection of proper α optical-model potentials. Drisko, Satchler, and Bassel[34] observed that potentials belonging to the same family differ from each other in that one additional half-wave length of each pertinent partial wave is pulled into the potential for successively deeper potentials. Therefore, the deeper the potential the more rapidly the associated partial wave oscillates inside the nucleus. In short, the deeper potential possesses the advantage of a reduced contribution from the nuclear interior.

The effects of different potentials on the theoretical angular distributions have been checked in detail by again using the $L=0$ and $L=5$ transitions. In Fig. 15 the local zero-range calculations, based on the three searched NEL sets listed in Table I, for the $(1g_{9/2})^2_{L=0}$ and the $(2p^{\pi}_{1/2}, 1g^{\nu}_{9/2})_{L=5}$ transfers are compared with the corresponding data. The solid curve represents the calculation with NEL Set 3, the dashed curve with Set 2, and the broken curve with Set 1. The two-nucleon f.f. are those without residual interaction. The $L=0$ calculation with Set 2 seems to indicate this to be the best set in that the locations and shapes of the stripping peaks past 60° are very well predicted by it; but it gives the strongest stripping peak at 20°, and no such peak exists there in the data. The gross structure of the measured angular distribution is best duplicated by the calculation with Set 3, the deepest potential set. The local zero-range cal-

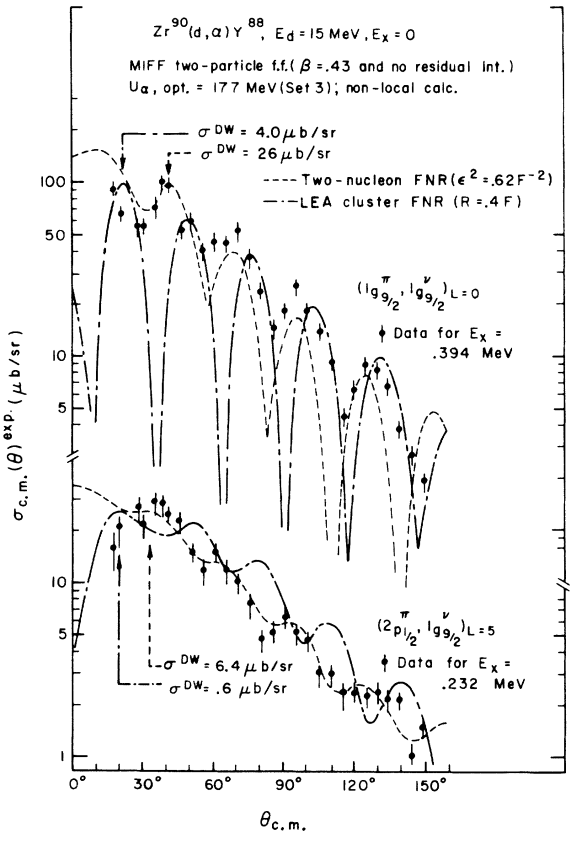

FIG. 14. Effect of the two different finite-range corrections shown in Fig. 13 on the cross sections. The same zero-range f.f. were used. Note the disagreements between the LEA calculations and the data.

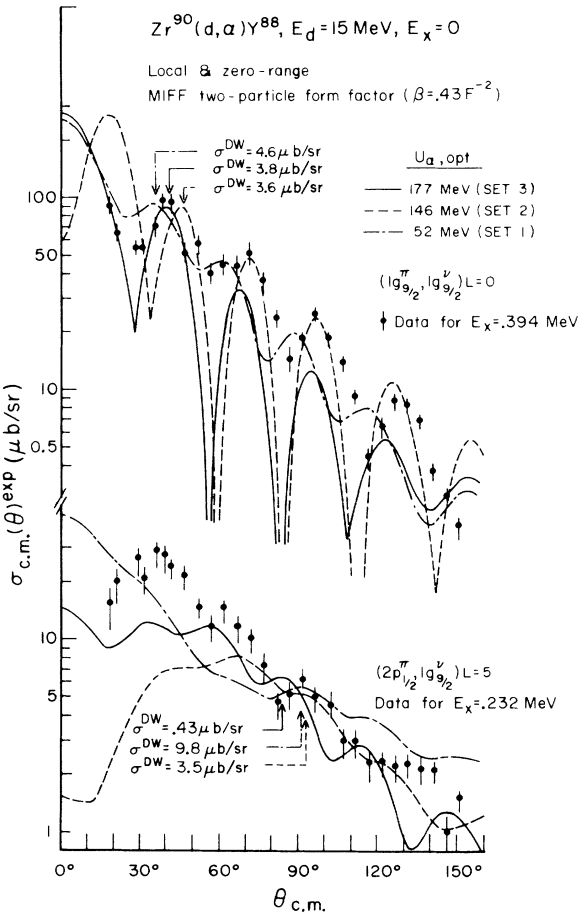

FIG. 15. Selection of the proper α potential set with local zero-range calculations. The calculations based on the three NEL α sets given in Table I and the same zero-range f.f. are compared with the data.

culations for $L=5$ lose their signature as is exhibited at the bottom of the figure.

It has been predicted that since the finite-range correction mostly affects the nuclear interior contributions, any feature which reduces the importance of these contributions also reduces the importance of the finite-range effect.[35] We then expect that the finite-range correction will improve the calculations very little when the deeper α potential is employed. In Fig. 16 the sensitivity check for the α potentials is repeated with calculations which include finite-range and nonlocality corrections. The definite superiority of Set 3 over the other two sets is quite evident for the case of the $L=5$ transfer. Also Set 3 gives better agreement with the $L=0$ data. By comparing the solid curves for the same L transfer in Figs. 15 and 16 the importance of the finite-range effect is clearly recognized even with the deepest α potential set, contrary to prediction. The fact that the finite-range correction influences the $L=5$ calculation far more than the $L=0$ calculation cannot be explained at the moment. Phenomena similar to this were also observed in the ^{68}Zn(d,α) reaction, where the correction drastically improved the $L=4$ calculation while the $L=2$ calculation was affected very little by the correction.[1] A recourse to the momentum mismatch argument given earlier in the (^{3}He, α) section suggests that the $L=5$ transition would be least affected by the finite-range correction because the momentum gap $|(M_f/M_i)L_d - L_\alpha| = 4$ created in the present (d,α) reaction is nearly spanned by the $L=5$ transfer.

(iii) Comparison between MIFF (Drisko-Rybicki) and DWUCK (Bayman-Kallio) form factors. The two-nucleon f.f., $f_L^\gamma(R)$, used in our (d,α) calculations were generated by the code MIFF of Drisko and Rybicki based on the oscillator expansion technique as mentioned earlier.[6] Here the problem of transforming the single-particle wave functions of a finite well to the relative and c.m. coordinates has been treated by first expanding the s.p.w.f. in terms of harmonic-oscillator wave functions of varying numbers of nodes and then performing the Talmi-Moshinsky transformation on the individual oscillator components.

Bayman and Kallio[36] have developed a different method for performing the transformation which deals directly with the finite-well wave functions and does not involve the harmonic-oscillator expansion. Their method is limited, however, to the case of the two-nucleon transfer with zero relative angular momentum. Since we assume the relative motion of the p-n pair in the α particle to be in a pure S state, it should be legitimate and interesting to compare the f.f. and the corresponding cross sections based upon them. The code DWUCK[26] includes an option to internally generate the two-nucleon f.f. based on the method of Bayman-Kallio. The s.p.w.f. are generated from a W-S well as in MIFF. DWUCK then calculates the two-nucleon f.f.

$$f^{\gamma}_{L,S=1}(R) = \left((l_p \tfrac{1}{2})_{j_p}(l_n \tfrac{1}{2})_{j_n} \middle| (l_p l_n)_L (\tfrac{1}{2}\tfrac{1}{2})_1)_J \frac{1}{R}\right.$$
$$\times \int_0^\infty r dr\, e^{-4\eta^2 r^2} f^L_{0,L}(r,R)\,, \qquad (15)$$

where $(\,|\,)$ is the JJ-LS transformation coefficient, and $f^L_{0,L}(r,R)$ is the distribution function with zero relative angular momentum.[36] The size parameter of the α wave function is η, as before.

In Fig. 17 unnormalized two-nucleon f.f. based on the two methods are shown for the $(1g_{9/2})_{L=0,\,J=1}$ and $(2p^{\pi}_{1/2}, 1g^{\nu}_{9/2})_{L=5,\,J=5}$ pure configurations. The solid curve represents the Drisko-Rybicki f.f. calculated by MIFF, and the dashed curve is for the Bayman-Kallio f.f. calculated by DWUCK. Both f.f. were generated from the same W-S single-particle parameters, and $\eta = 0.233$ F^{-1}. The MIFF f.f. have been multiplied by the transformation coefficients

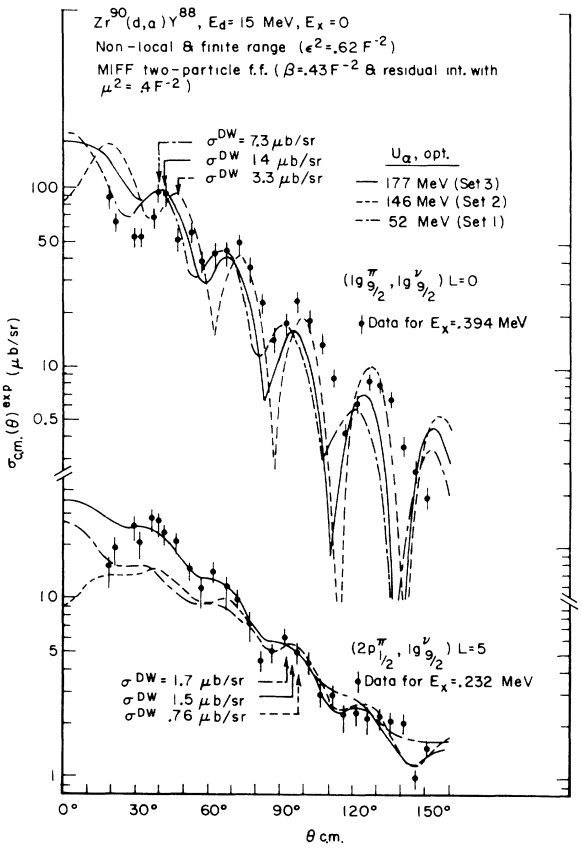

FIG. 16. Sensitivity check of the α potential sets with the nonlocal finite-range calculations. Note the over-all improvement in the theoretical angular distributions. Superiority of α Set 3 over the others is immediately clear.

since they are not included in MIFF. In the figure the DWUCK f.f. have been graphically normalized to the MIFF f.f. at $R=5$ F at which the magnitude of the DWUCK f.f. is indicated. Good agreement between the two f.f. is seen for both configurations as far as shape is concerned. A marked difference is observed in the magnitude for both configurations. The magnitudes of the DWUCK f.f. are smaller by a factor of 2.6 for the $L=0$ case, and by a factor of about 2 for the $L=5$ case at $R=5$ F.

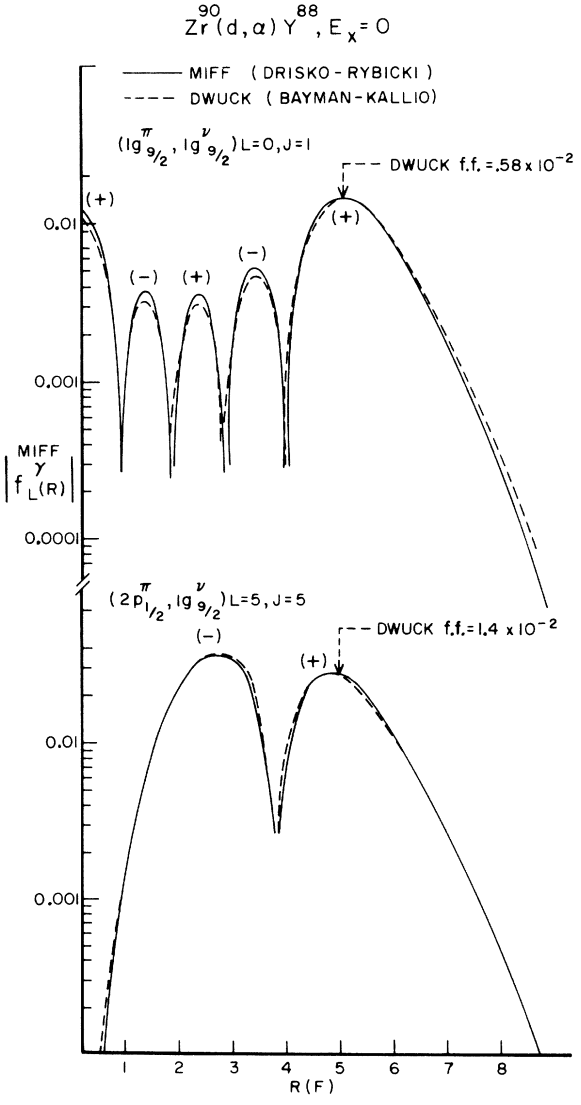

FIG. 17. Comparison of two-nucleon f.f. based on the Drisko-Rybicki method (MIFF f.f.) and the Bayman-Kallio method (DWUCK f.f.), both constructed from the same pure configurations. They have not been internally normalized to 1 prior to the calculation of the transition amplitudes. The scale on the left refers to the MIFF f.f., while the DWUCK f.f. is normalized to the MIFF f.f. at $R=5$ where the magnitudes of the DWUCK f.f. are specified.

The effects of these different f.f. on the local zero-range calculations are shown in Fig. 18. The solid curves stand for the calculations based on the MIFF f.f. and the dashed curves represent calculations based on the DWUCK f.f. The latter calculations are normalized to the former at the specified angles where the magnitudes of the DWUCK

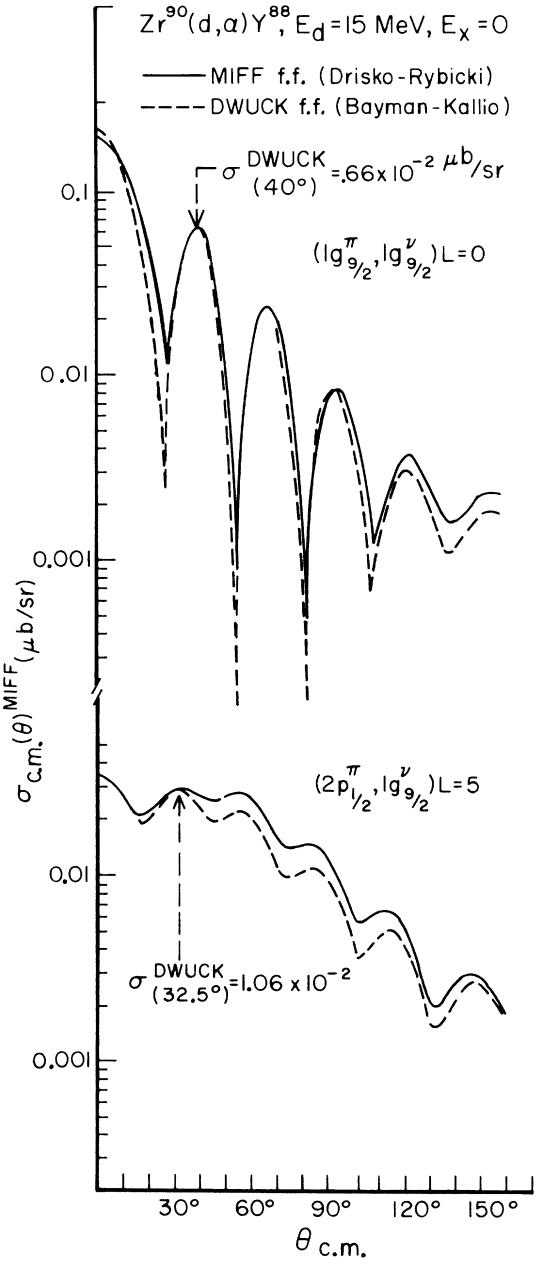

FIG. 18. Effect of the two different f.f. shown in Fig. 17 on the local zero-range calculations. The scale on the left refers to the calculation based on the MIFF f.f., while the cross sections based on the DWUCK f.f. are normalized to the MIFF f.f. at 40° for the $L=0$ transfer and at 30° for the $L=5$ case.

cross sections are indicated. We observe that the ratios of the cross-section magnitudes are well predicted by the square of the ratios of the corresponding f.f. magnitudes for both the $L=0$ and $L=5$ transfers. The minor discrepancy in the shape of the $L=0$ cross sections may easily be accounted for by the imperfect agreement in the shape of the corresponding f.f. in Fig. 17. The discrepancy in the slope of the $L=5$ cross sections, however, is unexpected because the two f.f. are practically identical, especially in the tail section, and because the $L=5$ calculations have shown little sensitivity to parameter variations. The difference in the effects of these two f.f. on the finite-range nonlocal calculations cannot be checked at the moment, because a two-nucleon finite-range formalism which could be used in conjunction with the Bayman-Kallio f.f. has not been reported. Results of a finite-range calculation on a (t, p) reaction based on a new formalism of Bayman have just been reported,[37] but the applicability of the formalism for a (d, α) reaction has not been tested in the present work.

(iv) Estimate of the (d, α) normalization. DWBA theories of direct two-nucleon transfer reactions have failed to establish the value of the absolute normalization D_0^2. Recently there have been attempts to empirically determine the value of D_0^2. Lewis and Daehnick obtained a value of $D_0^2 \simeq 20$ from the analysis of the ^{208}Pb$(d, \alpha)^{206}$Tl reaction.[30] This value, however, was obtained on the basis of nonlocal finite-range calculations in which the LEA finite-range correction was used. We have demonstrated that the use of this formalism is not justified in our analysis of the ^{90}Zr(d, α) reaction. Curry *et al.* gave $D_0^2(d, \alpha) \simeq 2$ from the analysis of the ^{31}P(d, α) reaction at 33 MeV.[38] They used the Bayman-Kallio f.f. in their calculations, while the Pittsburgh value is based on the Drisko-Rybicki f.f. Thus there is a need for further searches for a more realistic normalization; otherwise the extent of the usefulness of a direct (d, α) reaction to check the validity of the nuclear shell-model wave functions will be greatly limited.

An attempt was made to extract a value for D_0^2 from the present ^{90}Zr(d, α) data for the transitions to the 0.394- and 0.232-MeV states in ^{88}Y. The normalization was extracted from (13) where only the local zero-range calculations were used for σ^{DW}. Based on the normalized MIFF f.f. constructed from the pure $(1g_{9/2})^2_{L=0}$ configuration, we obtained a value of $D_0^2(Z.R.) \simeq 25$ for the transition to the 1^+ 0.394-MeV state. Assuming a $(2p^{\pi}_{1/2}, 1g^{\nu}_{9/2})_{L=5}$ pure configuration for the transition to the 5^- 0.232-MeV state, we obtained $D_0^2 \simeq 32$. $D_0^2 \simeq 20$–30 appears to be appropriate for both the $L=0$ and $L=5$ transfers.

This value for the (d, α) normalization constant does, however, depend on many parameters. The factors which might affect the value of D_0^2 are as follows: (1) The use of the finite-range nonlocal calculations in place of the zero-range local calculations would reduce the value by a factor of 4 to 5 for those configurations chosen; (2) choices of the $(2p_{1/2})^2_{L=0}$ configuration for the 1^+ state and $(1f^{\pi}_{5/2}, 1g^{\nu}_{9/2})_{L=5}$ for the 5^- state would not change the above range of D_0^2 quoted since σ^{DW} differ by less than 10% from those based on the chosen configurations; and (3) other factors not yet investigated in the current (d, α) study are the alternative choices for the α size parameter, the single-particle binding energies, and, most of all, the configuration mixing. In view of these and other uncertainties inherent in the present procedure to empirically determine D_0^2, the range of $20 \leq D_0^2 \leq 30$ quoted above should be used with caution.

IV. ASSIGNMENTS OF J^{π} VALUES

Detailed accounts of the procedures by which J^{π} assignments to levels of odd-odd nuclei can be achieved from comparative studies of direct (d, α) and single-nucleon transfer reactions have been previously reported.[1] Our criteria for J^{π} assignments or narrow J^{π} limits to levels of ^{88}Y are as follows: (1) the (^{3}He, α) spectroscopic strengths and $2J+1$ rule, (2) overlaps between the (d, α) J^{π} limits and those from the single-particle transfers, and (3) the strong selection rules inherent in a direct (d, α) transfer. The results of our assignments are summarized and compared with those from the recent Nuclear Data Compilation[32] in Table IV. The Nuclear Data source summarizes the various results for assignments of level energies and J^{π} values below 1.8-MeV excitation of ^{88}Y, which had been reported by the end of 1969. The main reaction sources for this compilation are ^{88}Sr(p, n), ^{89}Y$(p, d\gamma)$, ^{88}Sr(^{3}He, t), and ^{89}Y-(^{3}He, α) reactions. Since then extensive and more detailed investigations of the level structure of low-lying levels of ^{88}Y have been conducted with single- and two-particle transfer reactions,[10, 39, 40] and more recently with the ^{85}Rb$(\alpha, n\gamma)$ γ-decay work.[41]

Ground state. The ground state J^{π} is known to be 4^- as uniquely determined from β decay[32] to the 2^+ first excited state in ^{88}Sr. This assignment is confirmed from the present (^{3}He, α) and (d, α) reactions.

$E_x = 0.232$ MeV. The previous 5^- assignment[32] proposed from the neutron pickup reactions[8, 9, 16] is supported by our (^{3}He, α) analysis. It is consistent with our (d, α) J^{π} limit of 4^- to 6^- from a unique $L=5$ assignment. Together with the ground

state, this state is regarded as a member of the doublet belonging to the $(2p^{\pi}_{1/2}, 1g^{\nu}_{9/2})$ configuration.[9] This 5^- assignment together with the 4^- assignment for the ground state is in accord with the (^{3}He, α) prediction based on the $2J+1$ rule.

$E_x = 0.394$ MeV. This state is a 1^+ state as determined from γ- and β-decay works.[32] Our assignment of $l_n = 1$ in the (^{3}He, α) reaction is in agreement with those previous neutron pickup reactions which limit J^{π} to either 0^+ or 1^+. Recognition of an $L = 0$ transfer to this state in the (d, α) reaction, however, points to 1^+ because 0^+ to 0^+ transitions are prohibited in a direct (d, α) transfer. This state is most likely a member of multiplets belonging to the $(2p_{1/2})^2$ configuration, or possibly an admixture with the $(1g_{9/2})^2$ configuration for which the population of a state with $J^{\pi} = (\text{even})^+$ is prohibited in a direct (d, α) transfer.[2]

$E_x = 0.687$ MeV. This level is not seen in the (^{3}He, α) nor (d, α) reaction. Evidence from other reactions[32, 40, 41] indicates 8^+ for this level, thus explaining the absence of this level in the (d, α) reaction. This state would have to be the 8^+ member of the $(1g_{9/2})^2$ multiplet.

$E_x = 0.706$ MeV. The most controversy arises over this level. The Nuclear Data Compilation[32] tentatively assigned 1^+ on the basis that the previous (p, d) and (d, α) transitions to the level seen at 0.701 MeV were classified as $l_n = 1$ and $L_{(d,\alpha)} = 0$, respectively. In contrast, the population of the level in the present as well as the previous (^{3}He, α) reaction[8, 9] is not confirmed, as can be seen in Fig. 2. In our (d, α) reaction the level at 0.706 MeV is strongly populated (see Fig. 1). The corresponding measured angular distribution shown in Fig. 19 in no way resembles the strong structure characteristic of an $L = 0$ transfer. It can be fitted moderately well with either an $L = 2$ or $L = 3$ transfer. If the $L = 2$ were the correct assignment the dominant pair configuration would be either $(2p_{1/2})^2$ or $(1g_{9/2})^2$, from which the J^{π} limit would be 1^+ or 3^+. If on the other hand the $L = 3$ transfer were correct, then the state must be a negative-parity state with $J^{\pi} = 2^-$, 3^-, or 4^-. A Hauser-Feshbach

TABLE IV. Listing of level energies and J^{π} values or J^{π} limits assigned from this work in comparison with those reported recently in Ref. 32. The values in parentheses denote tentative assignments.

Ref. 32		Present work					
			^{89}Y(^{3}He, α)		^{90}Zr(d, α)		
E_x (MeV)	J^{π}	E_x (MeV)	$l_n(j_n)$	J^{π} limit	$L(d, \alpha)$	J^{π} limit	J^{π} assignment
0	4^-	0	$4(g_{9/2})$	4^-, 5^-	3	$2^- \rightarrow 4^-$	4^-
0.232	(5^-)	0.232	$4(g_{9/2})$	4^-, 5^-	5	$4^- \rightarrow 6^-$	5^-
0.393	1^+	0.394	$1(p_{1/2})$	0^+, 1^+	0	1^+	1^+
0.687	(8^+)		Not seen		Not seen		...
0.701	(1^+)	0.706	Very weak		2	1^+, 3^+	$(1^+, 3^+)$
					or 3	or $2^- \rightarrow 4^-$	or (2^-)
0.764	(0^+)	0.767	$1(p_{1/2})$	0^+, 1^+	Not seen		0^+
					or very weak		
0.84[40]	(5^+)	(0.84)	Not seen		Weak		...
0.97[40]	4^+		Not seen		Not seen		...
		(1.10)	Not seen		Weak		...
1.124		(1.13)	Weak		Weak		...
1.218		1.220	$1(p_{3/2})$	1^+, 2^+	Not seen		$2^+(1^+)$
					or very weak		
1.277		1.279	$1(p_{3/2})$	1^+, 2^+	0	1^+	1^+
		1.326	Not seen		(5)	$(4^- \rightarrow 6^-)$	$(4^-, 5^-, 6^-)$
		1.469	Not seen		...		...
		1.560	$1(p_{3/2})$	1^+, 2^+	...		1^+, 2^+
		Doublet					
		1.596	$1(p_{3/2})$	1^+, 2^+	...		$(1^+, 2^+)$
		1.705	$3(f_{5/2})$	2^+, 3^+	...		3^+
		1.754	...		...		...
		(1.82)	Very weak		(3)	$2^- \rightarrow 4^-$	$(2^-, 3^-, 4^-)$
		(1.90)	Very weak		Weak		...
		(1.95)	...		...		...
		(2.05)	...		Weak		...
		(2.12)	Very weak		(5)	$4^- \rightarrow 6^-$	$(4^-, 5^-, 6^-)$
		(2.20)	...		...		...
		(2.24)	...		...		...

calculation in the ^{88}Sr(p,n) reaction[42] suggests 2^-, which would be in accord with the $L=3$ (d,α) assignment. The ^{85}Rb$(\alpha,n\gamma)$ work[41] reveals the existence of a doublet with 9-keV separation around this energy. One member of the doublet identified at 706 keV is assigned 1^+, which would support the $L_{(d,\alpha)}=2$ assignment for the level seen in (d,α). The other member of the doublet identified at 715 keV has been assigned 6^+, and such a level would not be populated in the (d,α) reaction. The possibility of the existence of a third level around this energy with 2^- and belonging to the $(1f_{5/2}^{\pi}, 1g_{9/2}^{\nu})$ configuration cannot be ruled out on the basis of the present work alone.

$E_x=0.767$ MeV. The $l_n=1$ assignment obtained from the (p,d) and previous (^{3}He, α) work is confirmed in the present (^{3}He, α) work, which leads to 0^+ or 1^+ on the assumption that the $l_n=1$ transfer is associated with a $p_{1/2}$ pickup as discussed earlier in Sec. III B 3. The population of this level is not well recognized in the (d,α) reaction, thus pointing to the 0^+ assignment for the level. The $(\alpha,n\gamma)$ work[41] and the Hauser-Feshbach calculations[42] confirm this assignment. The level appears to be the 0^+ member of the doublet belonging to the $(2p_{1/2})^2$ configuration, the other member being the 1^+ state at 0.394 MeV. This is also supported by the (^{3}He, α) $2J+1$ rule.

$E_x=0.84$ MeV. This level is not populated in our (^{3}He, α) reaction and too weakly populated in our (d,α) reaction to obtain a meaningful (d,α) angular distribution. It has recently been reported that the state is strongly populated in the ^{87}Sr(^{3}He, d) and ^{88}Sr(^{3}He, t) reactions.[40] The state appears to be predominantly a proton particle state. The $(\alpha,n\gamma)$ work uniquely determines 5^+.

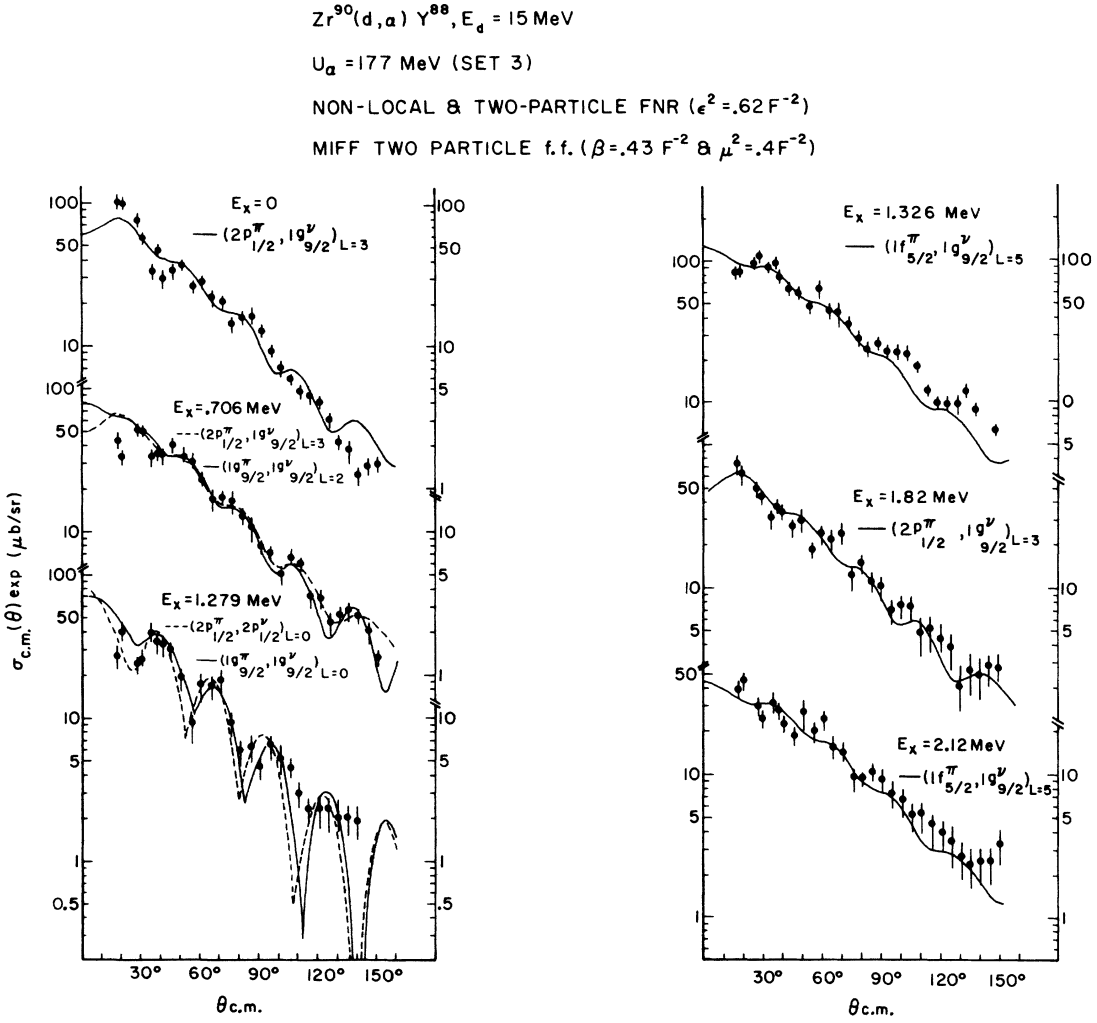

FIG. 19. The six remaining measured (d,α) angular distributions compared with the nonlocal finite-range DWBA calculations. A sufficient number of calculations were made so that the Q values of the data and curves do not differ by more than 0.5 MeV.

$E_x = 0.97$ MeV. This level, which has been known to be strongly populated in the $^{87}Sr(^3He, d)$ and $^{88}Sr(^3He, t)$ reactions,[40] is observed in neither the $(^3He, \alpha)$ nor (d, α) reaction. The state has been assigned 4^+ from the $(^3He, t)$ reaction, and it is interpreted as being the 4^+ member of the $(1g_{9/2})^2$ multiplet,[40] thus again explaining the absence of the level from our (d, α) reaction.

$E_x = 1.220$ MeV. Previous $(^3He, \alpha)$ studies[8,9] observed this level at 1.250 MeV, unresolved from a level at 1.306 MeV. In the current $(^3He, \alpha)$ analysis this level is identified at 1.220 MeV and is clearly resolved from the level at 1.279 MeV, which is the 1.306-MeV level in the previous work. The measured angular distribution for this level is well reproduced by the $l_n = 1$ transfer in Fig. 7, thus indicating 1^+ or 2^+ on the assumption that a $p_{3/2}$ neutron is picked up (see Sec. III B 3). This level is either not seen or very weakly populated in the (d, α) reaction, indicating that the state belongs predominantly to a $j_{J=\text{even}}{}^2$ configuration. In this case, the 2^+ assignment is favored. The $(\alpha, n\gamma)$ work[41] assigns 1^+ although a 2^+ assignment is not in conflict with the γ-decay scheme since the level feeds only the 1^+ 394-keV level.

$E_x = 1.279$ MeV. The $l_n = 1$ $(^3He, \alpha)$ transfer to this level is also likely to be a $p_{3/2}$ pickup transition, thus limiting J^π to 1^+ or 2^+. It is populated with moderate strength with an $L = 0$ transfer in the (d, α) reaction, thus limiting the choice to 1^+. The $(\alpha, n\gamma)$ work assigns 3^+ to a level at 1.284 MeV. Assuming that these two levels are indeed identical, the L value in the (d, α) transition to this level would have to be 2, 4, or a mixture of the two. Our $(1g_{9/2})^2_{L=2,4}$ calculations, however, do not possess the sharp structure exhibited in the measured angular distribution. A high-resolution (d, α) spectrum[12] indicates a doublet at 1.27 MeV with the two members being separated by less than 10 keV. It is possible that one member of the doublet is the 3^+ level assigned at 1.284 MeV in the $(\alpha, n\gamma)$ work. The 2^+ assignment suggested by the previous $(^3He, \alpha)$ works[8,9] appears to be incorrect.

$E_x = 1.326$ MeV. This level is not observed in the $(^3He, \alpha)$ reaction, but it is strongly populated in the (d, α) reaction. Our measured angular distribution is best reproduced by an $L = 5$ calculation in Fig. 19, leading to the J^π range of 4^- to 6^-. The $(\alpha, n\gamma)$ work tentatively assigns 6^- which is consistent with the above (d, α) J^π limits.

$E_x = 1.560$ MeV. This level is not resolved from the level at 1.596 MeV in our $(^3He, \alpha)$ reaction (see Fig. 2). A high-resolution spectrum[12] indicates that the level itself is a doublet with the two members being separated by less than 10 keV. An angular distribution has been obtained for this doublet hoping that the constituent levels would all be populated by the same l_n transfer in $(^3He, \alpha)$. In Fig. 7 the measured angular distribution compares well with both the zero-range and finite-range calculations for an $l_n = 1$ transfer. The identification of the $l_n = 1$ transfers to this group as $p_{3/2}$ pickup has been established earlier (see Sec. III B 3), and thus either 1^+ or 2^+ appears to be the most probable candidate for J^π. In the (d, α) reaction the unresolved doublet at 1.560 MeV is populated with moderate strength, which suggests a J^π value of 1^+. An assignment of 2^+ is possible if the state consists predominantly of the $(2p^\pi_{3/2}, 2p^\nu_{1/2})$ configuration, or an admixture of this with the $(1f^\pi_{5/2}, 2p^\nu_{1/2})$ configuration.

$E_x = 1.596$ MeV. The (d, α) spectra show this level as weakly populated, but perhaps not weakly enough to favor 2^+ over 1^+ on the basis of the strong (d, α) $j_{J=\text{even}}{}^2$ rule. Since firm evidence cannot be derived from the present work, the 1^+ or 2^+ assignment from the $(^3He, \alpha)$ reaction should be considered tentative.

$E_x = 1.705$ MeV. This level is populated strongly in the $(^3He, \alpha)$ reaction and moderately in the (d, α) reaction. The $(^3He, \alpha)$ transition is made by an $l_n = 3$, and this is most likely to be associated at this excitation with a $f_{5/2}$ pickup. In this case, J^π is limited to either 2^+ or 3^+. Since the population of the level is not inhibited in the (d, α) reaction, 3^+ is indicated.

Up to this excitation all the neutron single-particle strength available for the $l_n = 1$ and 4 pickup is virtually exhausted, and the strength for the $l_n = 3$ pickup has just begun to be detected. The fact that no prominent levels are observed beyond this energy in the $(^3He, \alpha)$ reaction clearly indicates that the $f_{5/2}$ and $f_{7/2}$ strength are widely fractionated. No attempt was made to obtain $(^3He, \alpha)$ angular distributions beyond this excitation. In contrast, levels are populated with considerable strength in the (d, α) reaction even beyond 3-MeV excitation. Because of the increasing level density, however, it became evident that a counter experiment with 30-keV resolution would not permit any further detailed analysis of odd-odd levels beyond this energy. It was therefore decided to obtain angular distributions to transitions only to levels at 1.82 and 2.12 MeV, both of which are strongly populated and appear to be sufficiently well resolved from nearby levels with comparable strength.

$E_x = 1.82$ MeV. This level is rather strongly populated in the (d, α) reaction with a tentative assignment of $L = 3$, giving $2^- \leq J^\pi \leq 4^-$. The level is either not seen or very weakly excited in the $(^3He, \alpha)$ reaction. This is expected at this energy, because a negative-parity state will not be populat-

ed until a neutron is picked up from the $2s$-$1d$ shell.

$E_x = 2.12$ MeV. The situation here is similar to that for the 1.82-MeV state, except that the (d, α) transition is tentatively identified as an $L = 5$ transfer, which yields a J^π range of 4^- to 6^-.

V. SUMMARY AND CONCLUSIONS

Emphasis was placed on detailed checks of the sensitivity to parameter variations of the DWBA calculations for the ^{89}Y(^{3}He, α)^{88}Y and ^{90}Zr(d, α)-^{88}Y reactions. The importance of the role played by the momentum mismatch condition in a (^{3}He, α) reaction[19] has received detailed study. Previous conclusions that the measured angular distributions for (^{3}He, α) transitions which proceed under momentum matching conditions are well predicted by conventional no-cutoff DWBA calculations have not been confirmed from the present work. Even for the case of momentum matching, we found that Stock's criterion for the proper potential combination[19] appears to be stringent only when the "modified" ^{3}He potential parameters are used in place of the conventional "measured" parameters derived from elastic scattering.

Based on the empirically determined (^{3}He, α) absolute normalization ($C = 25$) the spectroscopic factors were extracted using both the local zero-range and nonlocal finite-range calculations. The two sets of values agree within 10%. The finite-range and nonlocality corrections tend to smooth out the strong structure exhibited in $l_n = 1$ calculations not evident in experimental data.

The validity of the two-nucleon finite-range correction formalism of Chant and Mangelson[5] has been tested in detail for the ^{90}Zr(d, α) case. The two-nucleon f.f. calculated with the inclusion of the residual interaction (finite-range f.f.) are reduced in the nuclear interior by as much as an order of magnitude compared with those calculated without the interaction (zero-range f.f.) for the cases where the "angular momentum balance," $l_p + l_n = L$, is far from satisfied. The drastic reduction of the finite-range f.f. in the nuclear interior has different effects on the theoretical angular distributions for different L transfers. For $L = 0$ transfers, the main effect is to further smooth out the sharp structure present in the zero-range calculations and to decrease the cross section magnitudes by a factor of 2. For the $L = 5$ transfer the effect is negligible.

Attempts to simulate the finite-range f.f. by the "equivalent" cluster[1] f.f. were not, in general, successful because of the reduction of the former f.f. in the interior as mentioned above. The representation of the cluster f.f. equivalent to the zero-range f.f. is a poor one for the configurations where the angular momentum balance conditions are not met. We thus conclude that the use of the cluster f.f. in the (d, α) DWBA calculations is not, in general, justified.

The reliability of the extracted $L_{(d,\alpha)}$ transfers based on pure configurations has been examined. The over-all structure of the angular distributions is L characteristic. We attribute the imperfect reproduction of the measured angular distributions by the present calculations to the neglect of admixed configurations.

The validity of the application of the LEA finite-range correction[4] to the (d, α) case has been examined. The LEA finite-range calculations consistently failed to reproduce the gross structure of the data, even with the use of the best potential combination and the best range value of 0.4 F.[1] We conclude, therefore, that the application of the LEA finite-range correction to the (d, α) analyses should be avoided because of the inconsistency in results.

The well-known ambiguities in the α optical-potential sets did not present a problem in our (d, α) analysis as the selection of the proper set had been made prior to the analysis. The superiority of the set with the deepest real well over the other two sets searched was even more distinctly recognized with the finite-range correction included than otherwise. Contrary to prediction, we thus conclude that the use of a realistic finite-range correction is as important as is the correct choice of the α potential in the (d, α) DWBA calculations if the best theoretical reproduction of the data is to be obtained.

The previously proposed value, $D_0^2 = 20$, for the (d, α) absolute normalization[30] is in agreement with the limits of $20 \leq D_0^2 \leq 30$ determined with the use of local zero-range calculations in this work. The former value is based on calculations made with the inclusion of the LEA finite-range correction. The use of the more realistic finite-range correction would reduce each of our limits by as much as a factor of 5. We suggest, however, that the reliability of the empirically extracted value should be checked thoroughly with more refined calculations.

Although a qualitative agreement is seen between the Drisko-Rybicki f.f. (MIFF) and the Bayman-Kallio f.f. (DWUCK), the magnitude of the latter is consistently smaller by a factor of 2 to 3 for pure configurations. The use of the Bayman-Kallio f.f. in (d, α) DWBA calculations for reliable extraction of spectroscopic information from the data requires more stringent tests.

ACKNOWLEDGMENTS

The authors are grateful to Dr. D. Eccleshall for his interest in this work. We are obliged to Dr. A. W. Barrows, Jr., who participated in the initial phase of this work. The invaluable assistance of R. W. Gordon in the preparation of the scattering chamber and in accelerator operation is gratefully acknowledged. Also, the services of J. A. Morrissey and J. N. Mougianis for accelerator operation are acknowledged. We also wish to thank H. Crosby for preparing the figures.

[1]W. W. Daehnick and Y. S. Park, Phys. Rev. 180, 1062 (1969); Phys. Rev. Letters 20, 110 (1968); Y. S. Park, Ph.D. thesis, University of Pittsburgh, 1968 (unpublished).

[2]N. K. Glendenning, Phys. Rev. 137, B102 (1965).

[3]C. L. Lin and S. Yoshida, Progr. Theoret. Phys. (Kyoto) 32, 885 (1964); E. M. Henley and D. U. L. Yu, Phys. Rev. 133, B1445 (1964); I. S. Towner and J. C. Hardy, Advan. Phys. 18, 401 (1969), and references therein.

[4]P. J. A. Buttle and L. J. B. Goldfarb, Proc. Phys. Soc. (London) 83, 701 (1964); F. G. Perey and D. Saxon, Phys. Letters 10, 107 (1964).

[5]N. S. Chant and N. F. Mangelson, Nucl. Phys. A140, 81 (1970).

[6]R. M. Drisko and F. Rybicki, Phys. Rev. Letters 16, 275 (1966).

[7]R. DelVecchio, W. W. Daehnick, D. L. Dittmer, and Y. S. Park, Phys. Rev. C 3, 1989 (1971).

[8]C. M. Fou and R. W. Zurmühle, Phys. Rev. 176, 1339 (1968).

[9]G. Bassani and J. Picard, Nucl. Phys. A131, 653 (1969).

[10]Y. S. Park, H. D. Jones, and A. W. Barrows, Jr., Bull. Am. Phys. Soc. 15, 63 (1970).

[11]Y. S. Park, H. D. Jones, A. W. Barrows, Jr., and D. E. Bainum, unpublished.

[12]We are indebted to Dr. W. W. Daehnick for sending us the sample energy spectrum.

[13]R. K. Jolly, Ph.D. thesis, University of Pittsburgh, 1964 (unpublished).

[14]We are indebted to Dr. R. Shnidman for allowing us to use, with his assistance, his fitting program.

[15]The yttrium target was obtained on loan from the University of Pennsylvania; we are indebted to Dr. C. M. Fou for the loan.

[16]C. D. Goodman, Oak Ridge National Laboratory Report No. ORNL-4217, 1968 (unpublished).

[17]N. Austern, Ann. Phys. (N.Y.) 15, 299 (1961).

[18]G. R. Satchler, in *Proceedings of the Conference on Direct Interactions, Padua, Italy, 3–8 September 1962,* edited by E. Clementel and C. Villi (Gordon and Breach, Science Publishers, Inc., New York, 1963).

[19]R. Stock, R. Bock, P. David, H. H. Duhm, and T. Tamura, Nucl. Phys. A104, 136 (1967).

[20]We are indebted to Dr. F. G. Perey for permitting us use of the code JIB.

[21]M. R. Cates, Oak Ridge National Laboratory Report No. ORNL-TM-2426, 1969 (unpublished).

[22]L. McFadden and G. R. Satchler, Nucl. Phys. 84, 177 (1966).

[23]N. Austern, R. M. Drisko, E. C. Halbert, and G. R. Satchler, Phys. Rev. 133, B3 (1964).

[24]J. K. Dickens, R. M. Drisko, F. G. Perey, and G. R. Satchler, Phys. Letters 15, 337 (1965).

[25]F. G. Perey and D. Saxon, Phys. Letters 10, 107 (1964).

[26]We are indebted to Dr. Kunz for making the code DWUCK available to us and for providing us with a complete set of instructions.

[27]M. Krell, in Proceedings of the Symposium on Recent Progress in Nuclear Physics with Tandems, Heidelberg, Germany, 18–21 July 1966, edited by W. Hering (unpublished).

[28]J. B. French and M. H. Macfarlane, Nucl. Phys. 26, 168 (1961).

[29]See Ref. 19.

[30]M. B. Lewis and W. W. Daehnick, Phys. Rev. C 1, 1577 (1970).

[31]We are indebted to Dr. F. Rybicki for making the code MIFF available to us.

[32]Nuclear Data Compilation, C. D. Goodman, Bull. Am. Phys. Soc. 15, 572 (1970). We are grateful to Dr. Goodman for sending us the yet unpublished ^{88}Y level scheme.

[33]C. M. Perey and F. G. Perey, Phys. Rev. 132, 755 (1963).

[34]R. M. Drisko, G. R. Satchler, and R. H. Bassel, Phys. Letters 5, 347 (1963).

[35]R. M. Drisko and G. R. Satchler, Phys. Letters 9, 342 (1964).

[36]B. F. Bayman and A. Kallio, Phys. Rev. 156, 1121 (1967).

[37]B. F. Bayman, Phys. Rev. Letters 25, 1768 (1970).

[38]J. R. Curry, W. R. Coker, and P. J. Riley, Phys. Rev. 185, 1416 (1969).

[39]W. W. Daehnick and T. S. Bhatia, Bull. Am. Phys. Soc. 15, 572 (1970).

[40]R. C. Bearse, J. R. Comfort, J. P. Schiffer, M. M. Stautberg, and J. C. Stoltzfus; J. V. Maher, G. C. Morrison, and H. T. Fortune, Bull. Am. Phys. Soc. 15, 574 (1970).

[41]J. E. Glenn, H. W. Bear, and J. J. Kraushear, Bull. Am. Phys. Soc. 15, 1656 (1970). We are grateful to Dr. J. E. Glenn for sending us the ^{85}Rb(α,$n\gamma$) data prior to publication.

[42]G. C. Dutt and F. Gabbard, Phys. Rev. 178, 1770 (1969).